Adrian Oderwald Blazquez

Quality assessment of organic geotechnical samples

TUDelft

Quality assessment of geotechnical samples

By

Adrian Oderwald Blazquez

in partial fulfilment of the requirements for the degree of

Master of Science
in Geo-Engineering

at the Delft University of Technology,
to be defended publicly on Tuesday January 1, 2013 at 10:00 AM.

Supervisor:	Dr. Ir. Cor Zwanenburg	TU Delft
Thesis committee:	Kees-Jan van der Made,	Wiertsema & Partners
	Dr. Ir. Bram van den Eijnde,	TU Delft
	Dr. Karl-Heinz Wolf	TU Delft

This thesis is confidential and cannot be made public until October 12th, 2022.

An electronic version of this thesis is available at http://repository.tudelft.nl/.

TUDelft

Preface

Before you lies the thesis titled "Quality assessment of organic geotechnical samples", which is a report on the topic of geotechnical sampling disturbance. It was written to fulfil the graduation requirements of the MSc Applied Earth Sciences (track: Geo-engineering) at the TU Delft.

The entirety of the thesis was completed within 10 months. The literature study covers a large array of subjects, due to the abundance of sampling techniques and methods of assessing sample disturbance which have come to light in the past three decades. This thesis enabled me to achieve a high degree of understanding in a wide range of both geotechnical specific tests and experiments from other engineering areas. Data acquisition was particularly challenging, as the Netherlands was coming out of the COVID restrictions put in place which had diminished the usual high efficiency due to the pandemic regulations put in place. However, the positive attitude and willingness to help from the numerous individuals within the fields of my thesis enabled my research to be fruitful. The data collected by both Wiertsema & Partners and Deltares, and the data acquired by myself come from tests done exclusively on Dutch soils. In addition, the focus lies on samplers and sampling techniques used and/or developed in the Netherlands.

<div align="right">

Adrian Oderwald Blazquez
Delft, August 2022

</div>

Abstract

For certain geotechnical structures, such as dikes and levees, the design quality is heavily reliant on the sampling quality. In addition, the extent of consequences on geotechnical design of using parameters from samples with a certain degree of disturbance in laboratory tests is unclear. While the available literature has been mainly focussed on disturbance experienced by clay samples, the same empirical findings are not always applicable to organic soils such as peat and organic clay. The global objective of this thesis was to gain an understanding of sampling disturbance in organic soils using both established and non-destructive experimental methods. In order to achieve this, the traditional Dutch Ackerman sampling technique was compared to that of a recently developed sampler, the Deltares Large Diameter Sampler (DLDS). Non-destructive methods and 1D consolidation parameters were used to quantify disturbance in organic soil samples.

The results from existing databases showed that organic clay has a clear linear trend between w and RR and peat showed no definitive correlation, although the peat sampled by the DLDS had significantly higher water contents than the peats from the Ackerman sampler. Moreover, 37% of organic clay and peat Ackerman samples had an $\Delta e/e_0$ below 7%. Meanwhile, all the DLDS results from the Deltares laboratory had an $\Delta e/e_0$ of less than 4%. The use of this parameter is still questionable for peats, as the higher e_0 found in DLDS peats is the cause for low disturbance measurements. However, the $\Delta e/e_0$ index may be used in conjunction with other destructive and non-destructive disturbance parameters. Furthermore, the trend showed it becomes increasingly difficult to produce high quality samples with increasing in-situ vertical stress.

Using differences in shear wave velocity as a non-destructive disturbance determination technique, it was concluded that the increased shear wave velocity in Ackerman samples relative to the DLDS samples, although slight, was due to densification of the outermost volume of the sample being compressed by the sampling procedure. This effect was further observed in the other non-destructive method use in this investigation, CT scanning. Analysis of micro-CT scans showed that all specimens had higher greyvalue intensities at the perimeter than at the centre of the sample, however the observed effect was 7.4 times higher with the Ackerman specimens than with the DLDS specimens.

The main recommendation is to continue research on the effectiveness of using non-destructive methods to quantify sample disturbance in peats. For the sampling industry, it is advised to increase the diameter of the Ackerman sampling tubes to between 70 and 120 mm when sampling in peat. In addition, in light of the lesser disturbance caused by the DLDS, it is advised to deploy it in shallow peats instead of the Ackerman sampler with the current inner diameter of 67 mm. Furthermore, it is recommended to deploy both types of samplers side-by-side in sampling projects in order to diminish the effect of site-specific variables.

Table of Contents

List of Tables

List of Figures

List of Symbols

σ_v' = vertical effective stress

σ_v = vertical stress

OCR = overconsolidation ratio

CR = compression ratio

RR = recompression ratio

e = void ratio

e_0 = initial void ratio

C_i = inside clearance ratio

t_{100} = time to reach 100% primary consolidation

D/H = diameter to height ratio in oedometer cell

w = water content

V_s = shear wave velocity

V_{SCPTU} = shear wave velocity of soil measured by SCPTU

$V_{s,b}$ = shear wave velocity of sample measured in laboratory with bender element test

V_{vh} = shear wave velocity of sample measured in the field, immediately after sampling

$\Delta e/e_0$ = disturbance index

ε_{v0} = strain to load specimen back to in-situ effective stresses

$\Delta\varepsilon$ = strain increment

G = relative density (also named specific gravity)

γ_d = dry volumetric weight

γ_w = wet volumetric weight

σ_y = yield stress

Acknowledgements

First and foremost, I would like to thank my supervisors for their exceptional guidance during the duration of my thesis. Namely, my main supervisor and chair of my committee, Cor Zwanenburg who provided me with outstanding expertise, continued support and resources for my thesis. Kees-Jan van der Made gave me great insight into the industry-applied geotechnical knowledge and connected and supplied me with extensive resources of his company (Wiertsema & Partners). Karl-Heinz Wolf greatly guided me with the CT scanning and image analysis aspect of my thesis. As importantly, my gratitude goes out to Bram van den Eijnden, who significantly aided in structuring and organization of the report and provided attention to detail.

I'd like to thank all the staff at Deltares involved in my thesis for their time contribution in facilitating DLDS data and samples to me. Specifically, Harry van Essen provided me with said data in addition to providing insights into the challenges encountered with soil sampling. Dennis Pieters and Jeroen Ouwerling demonstrated and taught me the complex procedure of extracting samples from the DLDS.

Next, I wish to show my appreciation for the staff of Wiertsema & Partners. Egbert Wierenga helped enormously in coordinating apparatus availability during my time conducting tests at the company's laboratory and delivering this data to me. In this regard, Christiaan Koopman demonstrated and assisted me for a full day of bender element experimentation which proved vital to my work. Johan Bergsma and Jarmo Pietersen organized and provided me with the delivery of the STOWA data and oedometer data which was of high importance to my analyses. In addition, the help of Jordy de Vries, Ruben Geenen and Reke Talsma during the SCPTU fieldwork was phenomenal and crucial, given the complex acquisition system involved. In addition, the MASW field work would not have been possible without Mike van der Werf and Marco de Kleine, and their expertise and resources.

I wish to extend my thanks to the technical support staff of the TU Delft Faculty of Civil Engineering and Geosciences. Namely, the expertise of Ellen Meijvogel-de Koning in regards to executing CT scans and reconstructing them was invaluable. In addition, Roland Klasen and Cristina Cavero Panez provided me with oedometer testing guidance in the laboratory with exceptional ability, in addition to alternatives when necessary. Moreover, the reinforcement from Martijn Janssen with respect to image analysis is greatly appreciated.

Last but not least, I'd like to thank my parents for supporting me throughout the years of my studies. The level of encouragement is irreplaceable. In addition, I would like to thank my girlfriend Kate for cheering me on unconditionally throughout the full duration my thesis.

1 Introduction

1.1 Problem and research motivation

In the Netherlands, high safety standards must be met for water retaining structures such as dikes and levees, due to the catastrophic consequences that flooding imposes to the nation. As a result of the required safety standards, highly accurate stability analyses are necessary. In order to satisfy this, soil properties and geotechnical parameters used in stability analyses must be established from undisturbed geotechnical samples to represent in-situ conditions. Sample disturbance is defined as the damage to structure between particles in a sampled soil. Structural features include cementation, sedimentation, etc. The more disturbed a sample becomes, the less representative the derived parameters, from laboratory tests, are for in-situ conditions. Different sampling apparatus and methods induce different types and levels of disturbance. De-structuration and densification are examples of types of disturbance in soils. In general, the larger the sampler, the higher the volume of undisturbed material which may be retrieved. Friction occurs along the wall of samplers, which displaces soil along the surface. Therefore, the quality of the sample may not be the same throughout the sample.

Currently, it is challenging to explain to engineers and technicians why different sampling techniques must be used for different types of soil. Literature suggests that internationally used techniques such as piston and tube samplers have a higher degree of disturbance than newer methods used in Norway and the UK such as the Sherbrooke block sampler. However, the impact of the degree of disturbance on parameters is unknown. Consequently, sample disturbance has an influence on geotechnical design, but due to strict safety standards of water retaining structures, the impact is increased with respect to assessment of safety against flooding. Therefore, the problem statement is: in practice, lower quality samples, with some disturbance, are sometimes accepted for laboratory testing but the consequence on parameter accuracy is not fully known. National sampling guidelines of the Netherlands mention the use of different sampling techniques depending on the soil and required parameters, however, the large majority of sample are still being taken by the Ackerman sampler. These parameters are collected by independent waterboards in the Netherlands by the use of the Stichting Toegepast Onderzoek Waterbeheer (STOWA) databases. Therefore, more attention needs to be bought to using the most high quality method depending on the soil type and geotechnical parameters of interest, instead of innovating for high-speed methods. Subsequently, the consequences of using low quality samples for derivation of geotechnical parameters will be better established and accounted for.

It is of importance to distinguish the difference between samples and specimens; a sample is the entirety of the material extracted in the field within a recorded interval and stored within a container, while a specimen is the section of material withdrawn from a sample, prepared for a laboratory test. Presently, the most common type of sampling in the Netherlands is tube sampling with the Ackerman sampler, for any soil type. As an alternative for sampling in peats, the Deltares Large Diameter Sampler (DLDS) was developed by Deltares. This block sampler has considerably larger dimensions and the resulting samples are likewise increased in size compared to the Ackerman sampler. The DLDS was developed for shallow peats, however, as with the Ackerman sampler, it is possible to reach deeper soils with pre-drilling of the boring.

In order to validate the utility of using the DLDS and to ensure it meets the high standards for sampling peats, consolidation parameters resulting from oedometer testing will be compared to results from

traditional sampling methods and to a benchmarking method. The restriction of limiting the study to consolidation parameters derived from the incremental loading (IL) oedometer test is due to the importance of primary and secondary consolidation of peat, as it is abundant in the Netherlands, including in vital flood prevention structures such as dikes. Additionally, the aforementioned consolidation parameters are measured with relative ease in the Netherlands. Figure 1 shows evidence of the importance of correct sampling methodology due to the clear divergence in peak shear strength of heavily and low or non-disturbed samples.
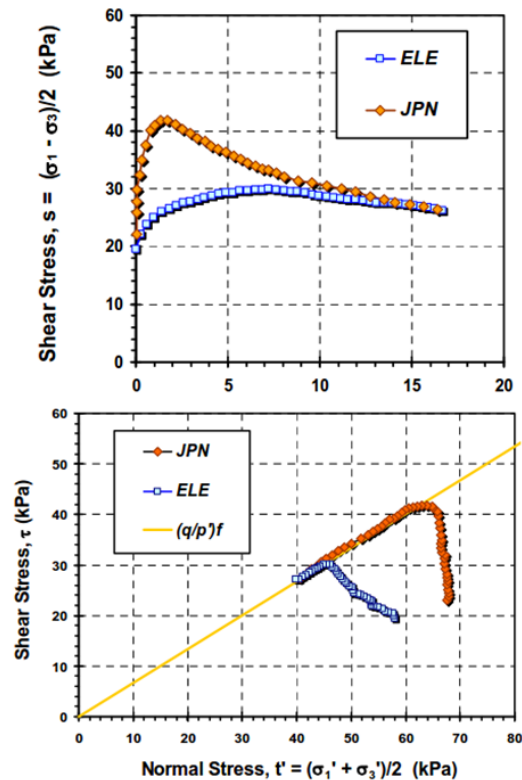
Figure 1. Triaxial test results on clay samples with different disturbance levels (ELE has more disturbance relative to JPN) showing the effect on the undrained stress-strain response (top) and the effective stress paths (bottom) (Mayne et al., 2009).

Samples of higher quality may not offer additional benefit, or samples of higher quality may only be necessary for certain soil types, geotechnical analyses or level of design. This is indicated in Figure 1, whereby the peak undrained shear strength differs up to 29% depending on the sampling technique used. The study is restricted to peat and organic clay, because these soils have been subject to lesser research regarding sampling disturbance. Additionally, organic clays have been included in this study as a basis of comparison because the behaviour of its plastic clay counterpart is well established.

1.2   Objectives

Main research question:
How does sampling affect soil properties and the consequent geotechnical design parameters?

Sub-question 1:
How does the DLDS affect consolidation parameters derived from (IL oedometer) laboratory tests in peats, when compared to traditional sampling techniques?

What is the relationship between sample disturbance and classification parameters (yield stress, density)?

Sub-question 3:
How do the properties (density and shear wave velocity) of organic clay and peat samples derived from CT scans and bender element testing* compare when different samplers are used?

Thesis objectives:
- Investigate the influence of the DLDS sampler on sample disturbance of peats.
- To gain an understanding to what extent consolidation parameters are affected by different sampling techniques.
- Establish possible differences in disturbance levels of samples from different samplers with CT scanning and bender element testing.

*serving as non-destructive disturbance assessment methods for comparison between different samplers.

1.3   Approach to answering research questions

Sub-question 1 will be partially answered by evidence gathered from the literature study. For the rest of the answer, data gathered from the Deltares DLDS database and IL oedometer tests performed at TU Delft on soil sampled by the DLDS will be compared to the database of STOWA which entails traditional techniques such as Ackerman sampling. Data gathered from the IL oedometer tests carried out for this study, and other (destructive) tests from which the results can be used to quantify sample disturbance, will form part of the Sample Disturbance Tests (SDT) database.

Sub-question 2 will be answered by IL oedometer tests performed at TU Delft and the available Deltares DLDS and STOWA databases. Regression analyses will be performed to determine the effect of disturbance on the geotechnical parameters from oedometer results.

In order to answer sub-question 3, computerized tomography (CT) scans will be used to make density distributions of samples sampled by the DLDS and Ackerman sampler. This enables distinction between different types of features of peat, namely branches, leaves, grass, etc. and account for the fibrousity of peat, which is a phenomenon that leads to higher sample disturbance compared to non-fibrous peat. The resolution of the medical-CT scanner is insufficient to distinguish discrete pores, causing an image with large amounts of interference. Therefore, the micro-CT scanner will be used in addition to the medical-CT scanner, to capture the densification disturbance type. The bender element testing will capture differences in shear wave velocity between sampled and in-situ soil as a measure of quality. Bender element testing and CT scanning have the benefit of enabling their use as alternative and non-destructive methods for quantifying sample disturbance.

The main research question will be answered after all sub-questions have been answered. By this point, a detailed understanding of sample disturbance will have been achieved whereby the changes in properties and design parameters resulting from disturbance will be explained. The interaction between

parameters (and therefore the antecedent research questions) can be seen in Figure 2, grouped by type of laboratory test, showing the link between each area of investigation.
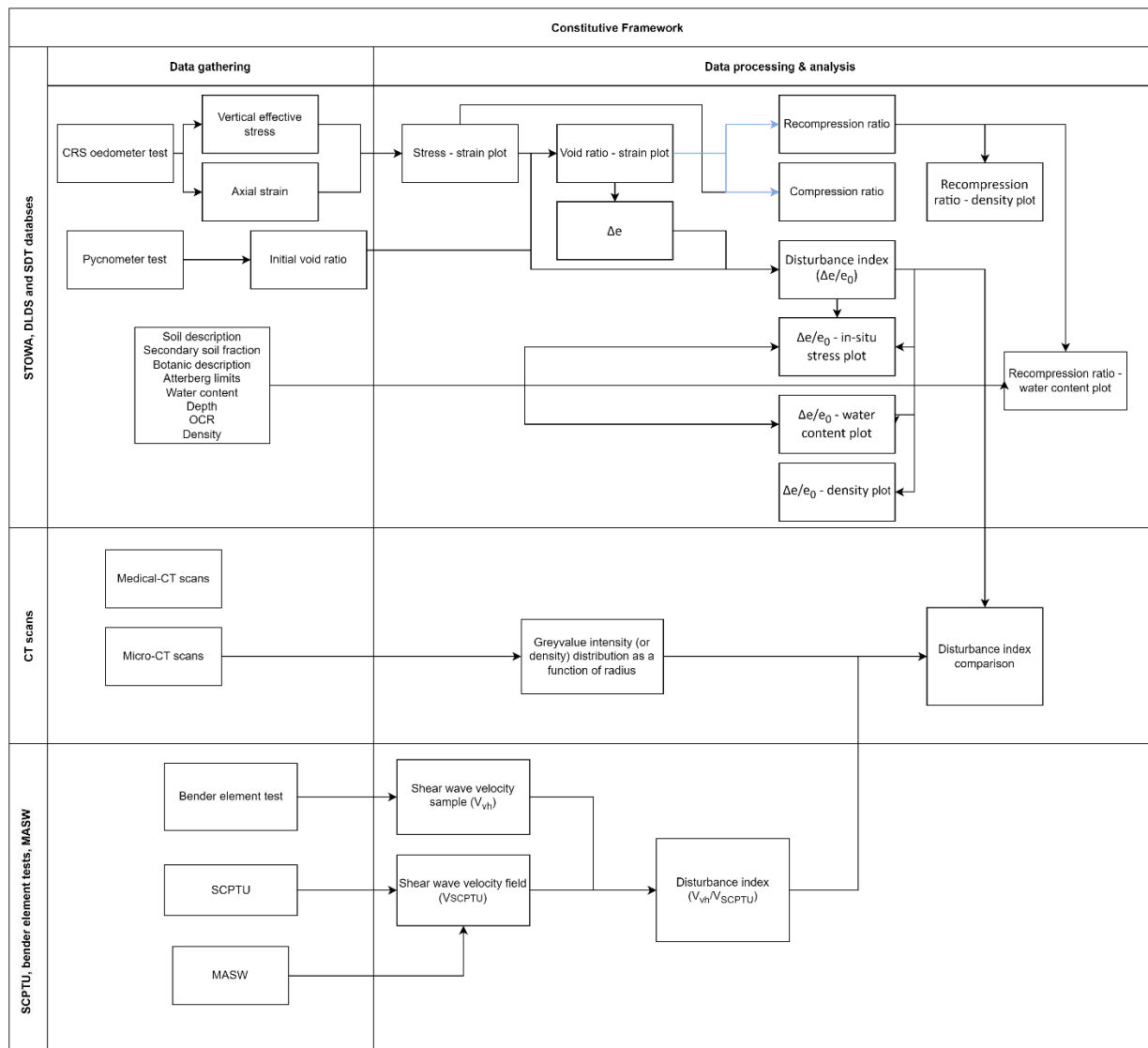
Figure 2. Constitutive framework of investigated parameters.

2 Background information

This section provides an overview of different types of samplers used to obtain soft soil samples. The focus lies on samplers used in Western Europe. Different categories for samplers exist depending on the sampling mechanism. The categories are block samplers, tube samplers and piston samplers. The necessity for different samplers exists due to strict standards in certain countries, such as the NEN-EN-ISO 22475-1:2021 (NNI, 2021). Additional sampler requirements are necessary in different soil types and soil conditions.

2.1 Block samplers

2.1.1 Sherbrooke block sampler

The Sherbrooke block sampler allows the carving of a cylindrical block with a diameter of 250 mm and height of 350 mm after pre-augering has taken place. Block sampling is ideal for sensitive, low plasticity clays which are heavily influenced by sampling disturbance (Lunne, 1997). Currently, it is widely perceived as the most effective method at retrieving an undisturbed sample. Nonetheless, for peats and soft organic clays bulging might occur, due to lack of lateral support during and after sampling. It has three cutting knives, which are fed with water from ground level in order to circulate the cuttings to the surface. A drill rod connected to the sampler allows for rotation while cutting (shown in Figure 3). With the use of a horizontal diaphragm installed in the Sherbrooke block sampler, the bottom of the carved block is removed from the in-situ soil (Lunne, 1997).
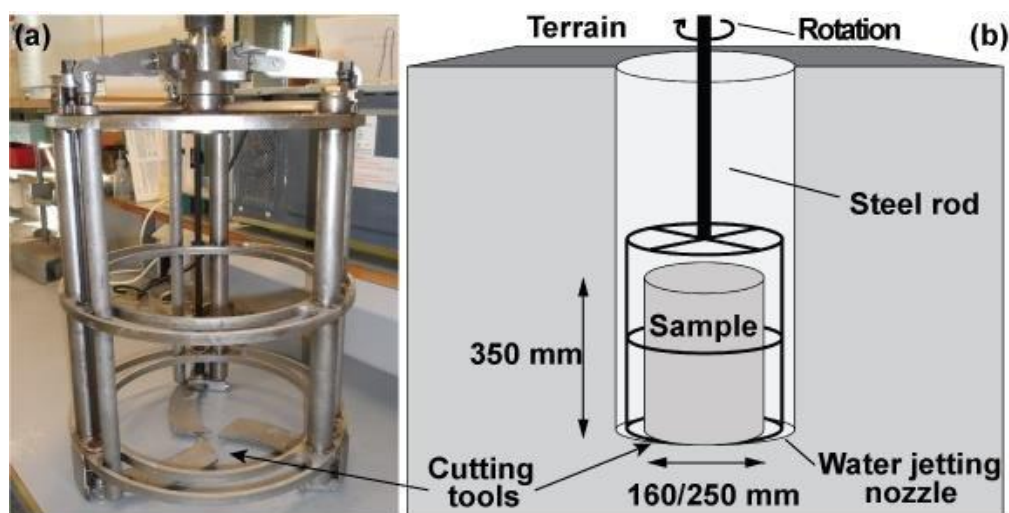
Figure 3. (a) Sherbrooke block sampler (b) schematic view of a block sample being carved (Amundsen et al, 2016).

2.1.2 Deltares Large Diameter Sampler

The Deltares Large Diameter Sampler was especially developed for use in soft soils with high organic matter content. Larger samplers often require additional measures to ensure minimal disturbance to the sample. In order to prevent bulging after sampling, the sample should have sufficient lateral support from the steel tube wall and it is sampled directly into its container as the sample is extracted from its in-situ position. Therefore, the Deltares Large Diameter Sampler (DLDS) was designed and developed

to be a tube sampler (Zwanenburg, 2017a). The down-hole sampler uses a casing to prevent collapse of the borehole after boring. The tube sampler consists of a cutting shoe, knives, the sample tube, a protection tube, a top cap and a plunger, configured as shown in Figure 4. The thickest section of the cutting shoe is 5 cm with a cutting edge of 10°. Before lifting the sample from the borehole, the knives provide a clean horizontal cut once the desired height of the sample has been reached. The sample tube is made of stainless steel with a diameter of 0.4 m, thickness of 3 mm and a variable height of 0.5 m or 1 m. A top cap allows for control of the knives, a connection to the plunger and a valve to let air and/or water escape when the sampler is pushed down. The valve is closed when extracting the sample in order to cause suction and prevent the sample from sliding down. Finally, the plunger uses six struts to securely fix the sampler during sampling (Zwanenburg, 2017a).
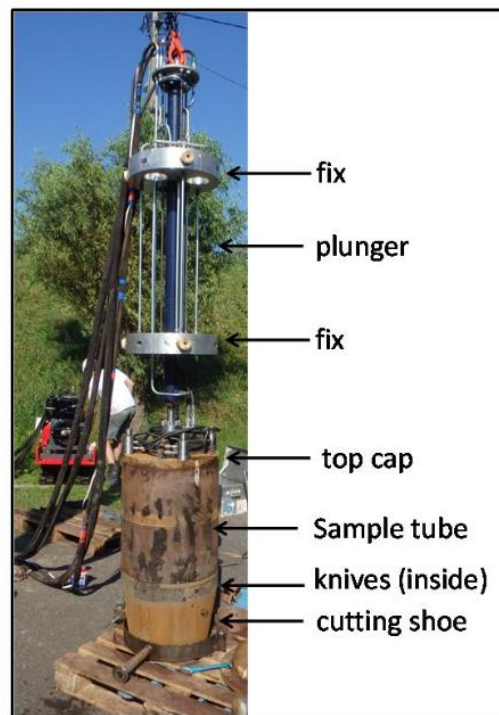
Figure 4. Components of the DLDS (Zwanenburg, 2017a).

Depending on the laboratory test to be performed, a different amount of block sampler can be prepared from a single tube. In the case of oedometer testing, from the total DLDS tube height variant of one metre, up to 16 block samples can be prepared. As the samples needed for triaxial testing are larger than oedometer samples, fewer samples can be prepared for this testing method. After the removal of 10 cm from the top of the tube, a cut is made every 20 cm, as shown in Figure 5, which is further divided into quarters as seen from a top view, making four equal blocks in the same dimensions. The bottom 10 cm is likewise discarded. These were then wrapped in a layer of plastic foil, followed by a layer of aluminium foil. The block samples are sufficiently protected from environmental effects in this configuration due to no loss of water to evaporation. The water content (w), which is a ratio of the weight of water to the weight of the solids in soil, does not diminish for these blocks, therefore the pore pressure remains constant, which results in a constant isotropic effective stress. As these stresses remain unchanged during storage, the volume remains constant which reduces susceptibility to disturbance.
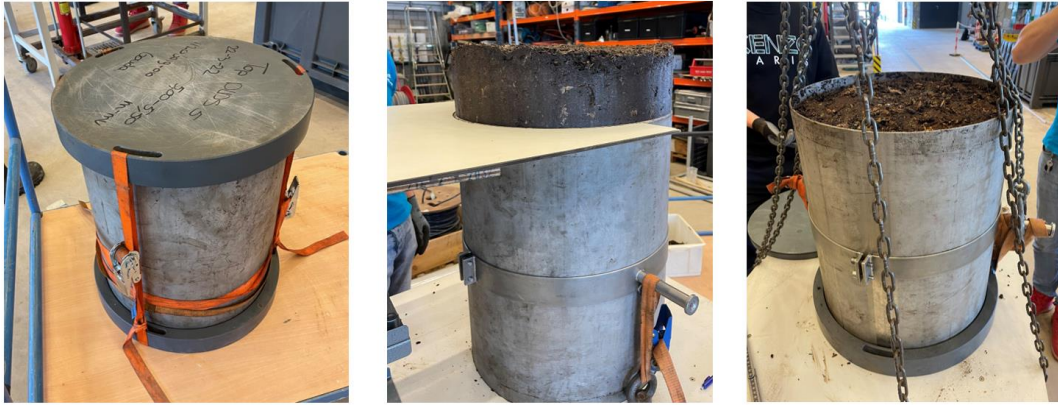
Figure 5. DLDS sample extraction from tube. The sample is provided with lateral and vertical support during storage (left), accurately cut during block preparation (middle) and secured by a crane during transport (middle).

2.1.3 Classical block sampling

The classical block sampling method entails the excavation of a circular trench around the intended sample volume. Then, it is trimmed of excess soil and wrapped in cheesecloth. Subsequently, it is covering with a thin layer of wax in order to retain the sample shape. This is followed by a wooden or metallic box being placed over the intended sample, as shown in Figure 6 (c). Lastly, using a wire, shovel, knife or saw (depending on the soil type), the base of the sample is detached from the surrounding soil. This sampling method is highly restricted by sampling depth, as it is not only economically unfeasible due to the increasingly large pit that needs to be excavated, but also due to the impractical matter of dewatering and intensive manual labour involved, as seen in the standard ASTM D7015/D7015M (ASTM, 2018).
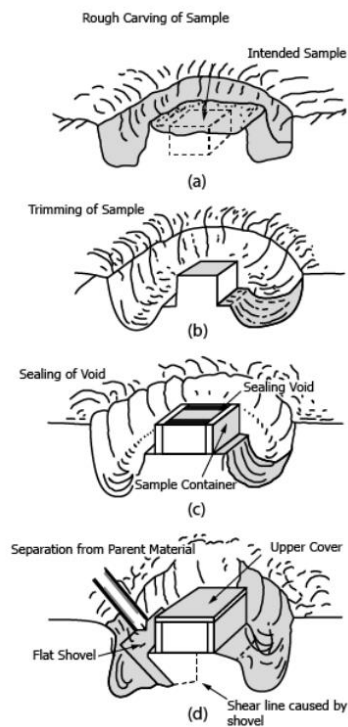
Figure 6. Classical (rectangular) block sampling method ASTM D7015/D7015M (ASTM, 2018).

2.2 Tube samplers

2.2.1 Ackerman sampler

The Ackerman sampler is the most commonly used sampler in the Netherlands. It is a thin-walled sampler producing a sample of at least 67 mm in diameter and 300 mm in length. This sampler is less suitable for sandy soils due to the need for core catchers, which cause the sample tube to remain fully or partially filled, simultaneously causing disturbance (TAW, 2001). In Dutch practice, the tube is hammered into the soil to obtain the sample and a recent study (Zwanenburg 2017b) concluded that using the static push method has no significant improvement on the results. Figure 7 shows a diagram of the sampler and its components. In this figure, the "stalen kogel" (translates to "steel ball" in English), is a device which allows for suction at the top of the sampler which results in reduced disturbance.
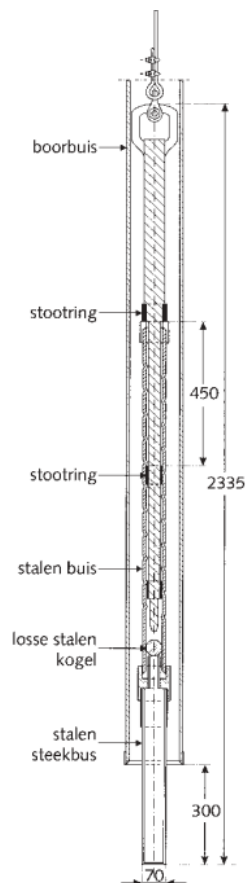
Figure 7. Ackerman sampler (sizes shown in mm) (TAW, 2001).

2.2.2 Laval sampler

The Laval sampler has a cutting edge of 5°, no inside clearance, 200 mm inner diameter, 218 mm outer diameter and (unlike other samplers) can be effectively operated in sandy soil under the water table. The sampler head has a central hole which allows for mud expulsion laterally from the sampling tube (Wride et al, 2000). Figure 8 (b) shows the operational procedure of the Laval sampler.
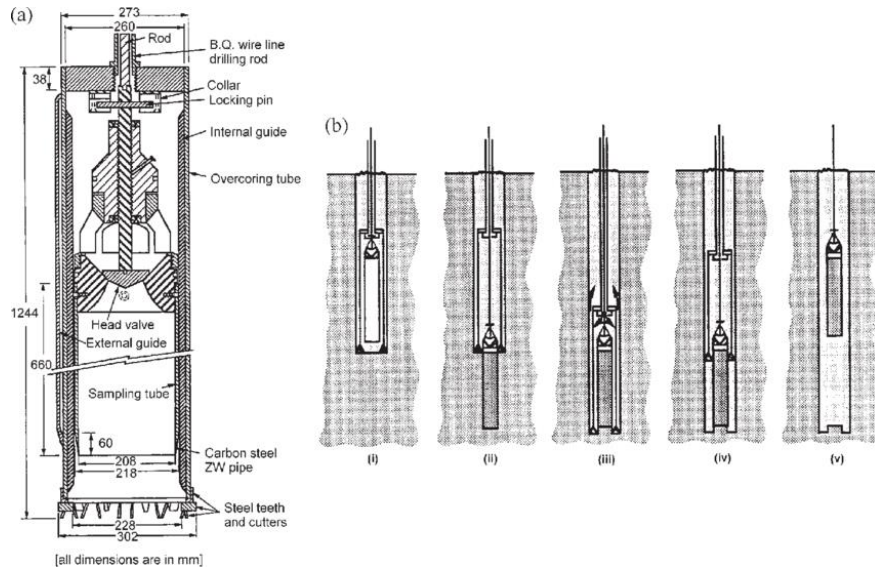
Figure 8. (a) Schematic of laval sampler (Konrad et al. 1995 and La Rochelle et al. 1981) and (b) cross-section of operational procedure (Konrad et al. 1995).

2.2.3 Holle Avegaar (hollow stem auger) sampler

The holle avegaar uses a pilot bit connected to a hollow tube with threads (auger) in order to drill into soil (shown in Figure 9). The diameter ranges between 60 and 100 mm, while a length of up to 6 m is possible. Once the sampling depth has been reached, the auger tube is held in place while the pilot bit is extracted and the sampling tube is inserted. Depending on the diameter of the auger tube, a sampling tube is inserted to extract the desired soil sample. The holle avegaar can be operated both over and under the water table, however in the latter condition the auger is to be filled with water before extracting the pilot bit (Nordmeyer, n.d.).
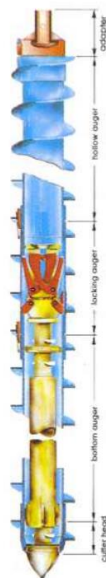
Figure 9. Holle avegaar diagram (Nordmeyer, n.d.).

2.3 Piston sampler

The piston sampler is a tube-like sampler, however it uses a piston to actively create suction at the interface between the piston and top of the sample, as shown in Figure 10. This means that piston samplers can only be used in soils which are below the water table. The piston remains static as the outer tube is pushed into the soil. Newer piston samplers may include a vacuum breaker, which reduces suction between the sample and piston during disassembly. Piston samplers exist in different diameters, for example the Norwegian Geotechnical Institute (NGI) 54 mm and NGI 95 mm (Lunne, 1997).
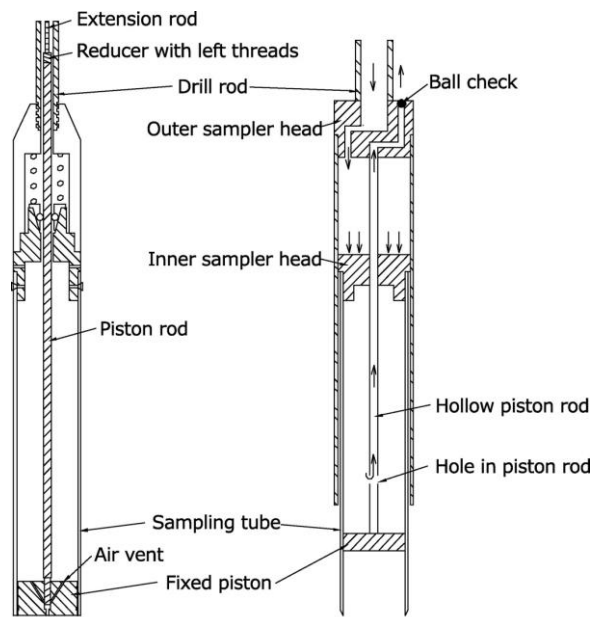
Figure 10. Piston sampler diagram (Chung, 2013).

3 Literature study

In this chapter, the available literature on sample disturbance is presented. First, the causes of sample disturbance are described. This section is followed by studies conducted on the influence of sample disturbance on soil properties and parameters. Thereafter, the current standards and guidelines are presented. Finally, the indices and methods used to quantify the level of disturbance described.

3.1 Causes of sample disturbance

Sample disturbance is caused by de-cementation of soil particles from external interference of in-situ soil leading to either volume reduction or increase. Long term/inappropriate storage can lead to disturbance due to loss of suction in the sampling tube, escape of humidity and therefore ultimately causing disturbance as the soil compacts. Soils with organic matter have degradation via aerobic and anaerobic degradation, which may cause chemical changes in the soil. Factors causing sampling disturbance are grouped into several categories such as the geometry of the sampling apparatus, volume displacement of the sample and the soil type being sampled. The inside clearance ratio (C_i or ICR), which is defined as the difference between the inside diameter of the sampling tube and the inside diameter of the cutting edge (Baligh et al., 1987) has the equation shown below (equation 1). This is shown in the schematic of Figure 11. In the case that $C_i > 0$, the soil experiences swelling in the cutting shoe at the centre-line of the sampler.

$$C_i = \frac{D_3 - D_1}{D_1} \tag{1}$$
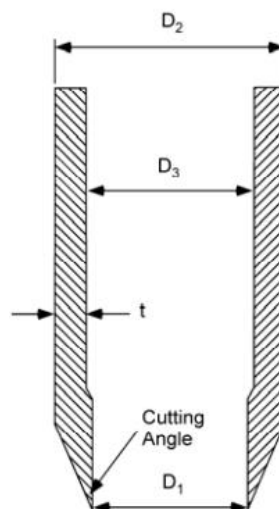
Figure 11. Sample tube dimensions (DeGroot et al, 2005).

The ratio of the sample height over tube height is called the recovery ratio (in Dutch: "steekverlies", however this is the inverse of the recovery ratio) and is of crucial significance in determining disturbance. This is due to the fact that the unfilled volume in the tube allows for the sample to lose its structure during transport and storage. Inversely, if the thrust distance is equal to the tube length, but only a fraction of soil length is present in the tube, the soil has been compressed by the equivalent empty

length of the tube. Commonly, Ackerman samples have a low recovery ratio, averaging 72% for when the Ackerman sampler is statically pushing into soil and 65% when the Ackerman sampler is hammered into soil (Zwanenburg, 2017b). This means that, often the top of the sampling tube does not contain the sampled soil. Ideally, the recovery ratio is close to 100%, in order to avoid movement of the sample material within the tube. Instead, this would-be void is mitigated by filling the remaining volume with a watertight bag containing sand. This practice could cause compaction of the sample, and therefore disturbance due to the added vertical stress (σ_v). For both the Sherbrooke and DLDS the sampling loss is negligible (Zwanenburg, 2017a).

Figure 12 is a sketch of a representative stress path of clay samples during sampling and specimen preparation proposed by Ladd and DeGroot (2003). A similar stress path is expected with regard to peat. Path 1-2 forms a significant cause of sample disturbance induced by reduction of σ_v (Ladd and DeGroot, 2003). In path 2-3, the increase in deviatoric stress (q) is attributed to a geometric factor of the sampler, the C_i, being greater than zero.
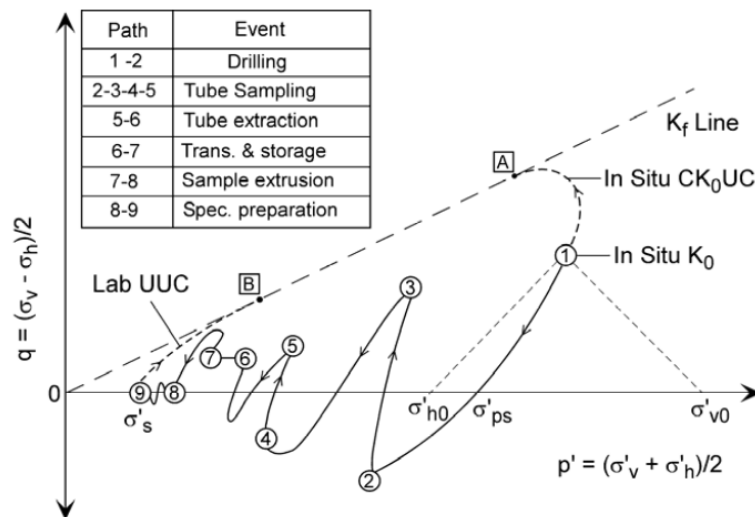
Figure 12. Centre-line stress path representation during sampling and specimen preparation of clay in tube samples (Ladd and DeGroot, 2003).

Swelling and compression during sampling, which is in the category of volume displacement, is represented by paths 3-4 and 4-5 respectively (Ladd and DeGroot, 2003). After the soil has passed the cutting shoe it enters the tube. In the case that the $C_i > 0$, the entering soil swells due to the newly available volume and lack of confining pressure. Due to the tendency of swelling for soils which experience reductions in confining pressure, a complication arises whereby some samples might get stuck in a tube with a $C_i = 0$. Disturbance might then occur when pushing out the sample back out when needed.

Path 5-6 is subject to suction during extraction of the tube (Ladd and DeGroot, 2003). The sudden change in stress as the soil under the cutting edge tries to resist the extraction of the sample can result in disturbance of said sample. Finally, path 6-9 represent the least sample disturbance potential, i.e. transportation, storage, handling and preparation of the sample (Ladd and DeGroot, 2003). A study by Tanaka (1996) confirmed that transportation and storage represent a very minimal portion of total disturbance. The study included clay transported from Drammen, Norway, for unconfined compression tests, to two very distant locations: the Norwegian Geotechnical Institute (NGI) and Port and Harbour

Research Institute (PHRI), in Japan. The same personnel and test procedures were used in both locations and it was found that no systematic difference was present in the results (Tanaka, 1996).

The area ratio (AR) is exclusively used for the cutting shoe, whereby it is defined as the difference between the square of the outer and square of the inner diameters, expressed as a ratio by division of the inner shoe diameter, as shown in Figure 13. Furthermore, the outside cutting edge angle (OCA) and inside cutting edge angle (ICA) are additional parameters used to classify tube samplers. The finite-element method (FEM) has been used to quantify disturbance from the centreline of the sampler and assess the influence of tube sampling via assessment of the influence AR, cutting edge angles and ICR (Clayton et al., 1998). FEM results were used as a comparison to analytical computations. The study concluded that an increase in the thickness of the sampler wall and therefore an increase in the area ratio of the sampler, caused a significant increase in the peak compressive strain during sampling. This can be seen in Figure 14, where an increasing AR increases the degree of axial strain in both compression and extension zones of the simulated soil. Additionally, it was concluded that an increase in the C_i caused an increase in peak strain in extension, similarly described as a cause of disturbance by Ladd and DeGroot (2003) and the increasing of the cutting edge angle marked an increase in peak compressive strain during sampling (Clayton et al., 1998).

- Outside cutting edge angle (OCA), α

- Inside cutting edge angle (ICA), β

- Inside clearance ratio (ICR), which controls internal friction:

$$ICR = \frac{D_s - D_i}{D_i} \qquad [1]$$

- Area ratio (AR), which relates the volume of displaced soil with the volume of the sample:

$$AR = \frac{D_e^2 - D_i^2}{D_i^2} \cdot 100 \qquad [2]$$
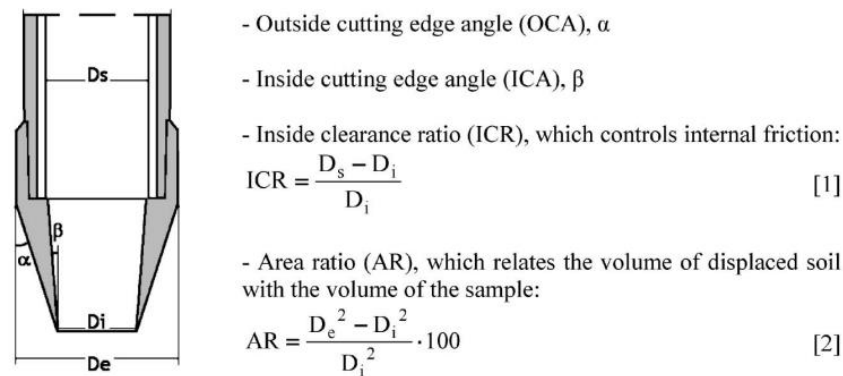
Figure 13. Definition of geometric parameters of tube samplers (Ferreira et al., 2011).
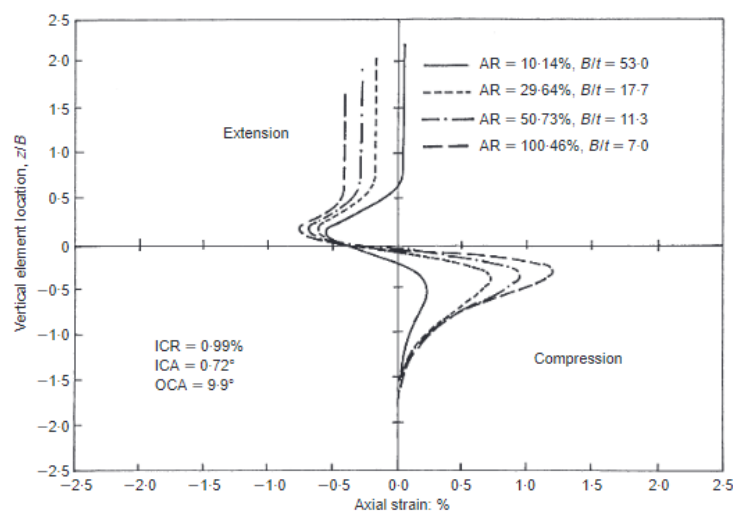
Figure 14. Centre-line strain paths for tube samplers with different area ratios (AR) (Clayton et al., 1998).

Helenelund et al. (1972) used thin-walled sampling tubes, with varying types of cutting edges to sample peats. In the paper, it was concluded that considerable compression of fibrous peats takes place regardless of the type of cutting edge. Therefore, the (pre-compressed) peat samples have adopted different properties than in in-situ conditions (Helenelund et al., 1972). Logically, this suggests that, in relation to sample disturbance, distinctions are required, regarding the type of peat. As observed by Helenelund et al. in 1972, peats with low fibrousity experience lower pre-compression by the cutting edge, while the opposite is true for peats with high fibrousity. The authors of the aforementioned paper recommend the use of a sawtooth shape cutting edge when sampling peats and rotary motion to increase the chance of cutting cleanly through peat fibres.

3.2   Influence of sample disturbance on soil properties and parameters

A newly developed block sampler, the DLDS, showed improvements compared to the Sherbrooke block sampler. Zwanenburg (2017a) stated that, from a study on using the DLDS to sample peat and organic clays, water content was higher when compared to the Sherbrooke block sampler. In addition, it was reported that the ratio between the compression ratio (*CR*) to recompression ratio (*RR*) was higher as well. The CR is used to quantify the compressibility of the soil, while the recompression ratio is a parameter calculated during a reloading stage of the 1D consolidation test, proceeding the lowering of a load. Lower density and lower normally consolidated stiffness were observed compared to the Sherbrooke block sampler. No clear difference could be observed in pre-consolidation stress. It is important to note that the size of the dataset was insufficient to draw final conclusions. While it is unclear how disturbance distributes within samples, only the outermost 'skin' of the sample might be affected. Therefore, increasing the diameter of a sampler ensures a greater undisturbed volume of the sample. This is an additional benefit of the DLDS, which has a diameter of 400 mm compared to the 250 mm in diameter of the Sherbrooke block sampler. A complication arises when measuring disturbance in peats, as a small change in void ratio (*e)* does not necessarily imply little disturbance due to the high compressibility of peat (Zwanenburg, 2017a).

Amundsen et al. (2015) conducted CRS oedometer tests on clay using block sampling and tube sampling of different diameters (75 mm and 54 mm). The results displayed in Figure 15, clearly show differing σ_v' paths depending on depth and sampler used. Furthermore, the constrained modulus likewise showed differences between depth and sampler used, notably peaking at differing σ_v'. The constrained modulus depends on the deviator and mean effective stress, therefore horizontal and vertical stresses were largely different for each sample type.
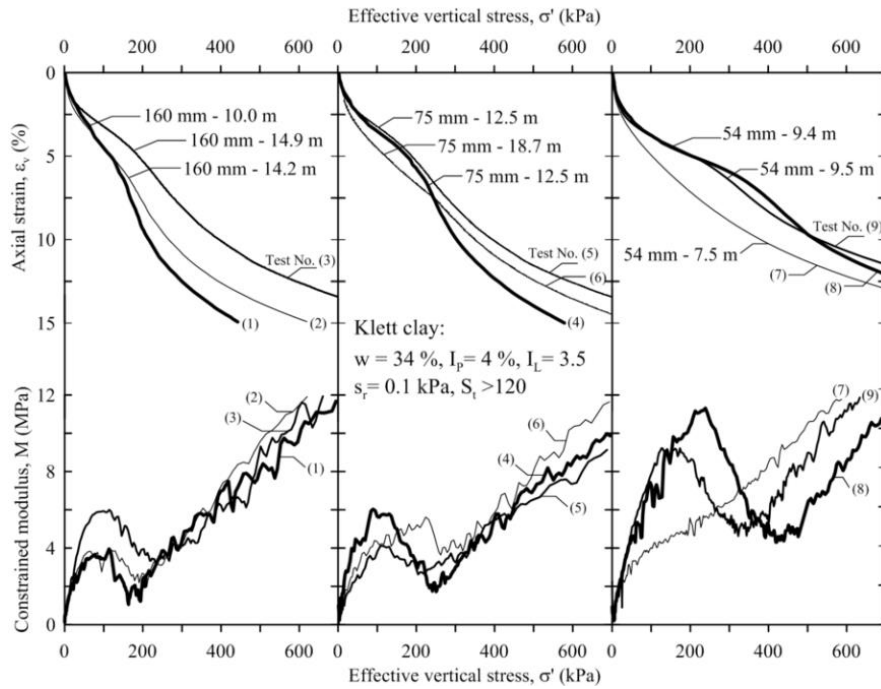
Figure 15. Oedometer tests on block and tube samples from Klett, Norway (Amundsen et al., 2015).

From Figure 15, it can be identified that the strain response for tube samples (middle and right graph) showed a stiffer response compared to the block sample (right). This is especially the case for the 54 mm sampler results (right), since a significantly higher σ_v' is needed to achieve the same axial strain, for samples from the same depth. This indicates that the tube samples have been subjected to compaction during sampling, hence a higher degree of disturbance compared to the block sample results.

The influence of sample disturbance on compressibility properties on peat were investigated in a paper by Helenelund et al. (1972). It was noted that the thin walled tube samples showed a stiffer response than the block samples due to the densification they had undergone during sampling. The paper concluded that using conventional thin walled tubes resulted in 2.5 times higher peak strength compared to block sampling. This is in contrast to the finding for clays by Mayne et al (2009), which showed the clear divergence in peak shear strength of samples with varying degrees of disturbance. This further alures to the importance of sampler selection depending on the soil being sampled. Figure 16 shows CRS testing done on clay samples by Lunne et al. (1997) graphed on a logarithmic scale for effective axial stress, whereas Amundsen et al. (2015) used a linear scale as seen in Figure 15.
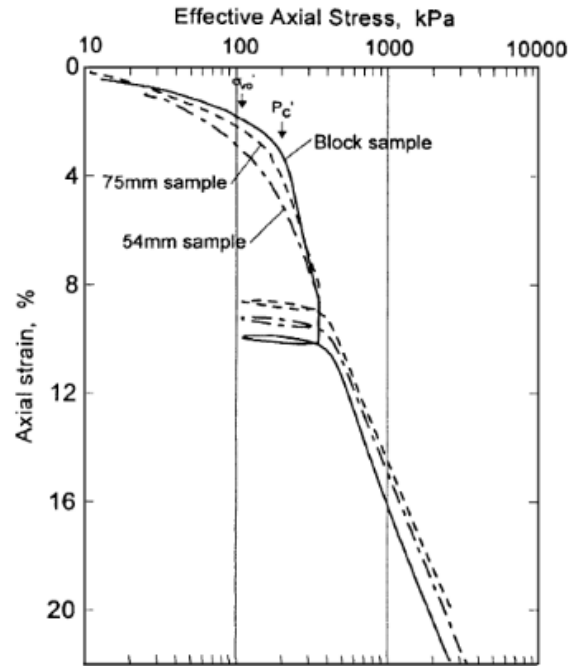
Figure 16. CRS tests on Lierstranda clay (Lunne et al., 1997).

Boylan (2008) conducted CRS oedometer tests in the Netherlands on sampled peat via Sherbrooke block sampling, piston and hollow auger sampling. He noted that piston and hollow auger sampling showed a higher initial stiffness than the block sample. Both the disturbance index $(\Delta e/e_0)$ and modulus number were used as sample quality criteria. The former showed that piston and hollow auger samples appear of higher quality than the block samples, which is attributed to the high overconsolidation ratio (OCR), much higher than the limit of 4 of this criteria, of these samples and the densification effects. In contrast, using the modulus number, it was concluded that since the piston and hollow auger samples have a higher modulus number, they are less compressible than the block samples. In addition, it was concluded that, similar to Zwanenburg (2017a), the disturbance index based on the normalized Δe is misleading for peats, when densification has occurred. In the case that the DLDS does not lead to densification of the sampled soil, and the peat is of appropriate OCR, the $\Delta e/e_0$ may be used to assess the sample quality. Finally, the study by Boylan (2008) indicates that peat samples with high w (>500%), will lead to water migration in the sample during storage, resulting in an increased w at the bottom and a decreased w at the top of the sample.

3.3 Standards and guidelines

Certain samplers can only achieve limited sample quality as detailed in the ISO standard ISO-22475 (NNI, 2018). This classification is found in Table 1. High sample quality is necessary, i.e. Class 1 samples, for tests which rely on quantification of strength and structural features of soil, such as triaxial and oedometer testing. Only corresponding sampling methods which fall under Category A may be used to obtain these samples. With the categorization as presented in Table 1, it demonstrates that, for example, it would be poor engineering practice to use methods from sampling category E to aim to obtain particle size from samples.

Table 1: Quality classes of soil samplers for laboratory testing and sampling categories (NNI, 2021).

Soil properties	Quality classes of soil samples for laboratory testing				
Unchanged soil properties	**1**	**2**	**3**	**4**	**5**
particle size	*	*	*	*	
water content	*	*	*		
density, density index, permeability	*	*			
compressibility, shear strength, stiffness	*				
Properties that can be determined					
sequence of layers	*	*	*	*	*
boundaries of strata - broad	*	*	*	*	
boundaries of strata - fine	*	*			
Atterberg limits, particle density, organic content	*	*	*	*	
water content	*	*	*		
density, density index, porosity, permeability	*	*			
compressibility, shear strength, stiffness	*				
Sampling categories	A				
		B			
			C		
				D	
					E

The ISO standard, ISO-22475 (NNI, 2018) describes Class 1 samples to be suitable for oedometer testing. Class 1 samples can only be achieved through category A sampling methods. Samples from Class 2 to Class 5 are suitable only for tests where de-structuration of the sample less important. This leaves a restricted number of sampling methods that may be used for oedometer tests. As seen in article 6.3.1.4 of the standard, rotary drilling is the only method by which boreholes should be made to sample peat. For organic clays, there are additional methods which can deliver Class 1 samples such as hammer driving and rotary hammer driving. Table 2 shows the samplers which must be used to sample certain soil types to achieve varying sample qualities. As shown, thin-walled tube samplers of 70 to 120 mm diameter, and in rare cases thick-walled tube samplers of 50 to 100 mm diameter, are appropriate for sampling organic clays and peats for category A samples. However, the 67 mm inner diameter of the thin-walled Ackerman sampler falls just short of this requirement, therefore categorizing into line 3 of Table 2, with the appropriate length variants.

Table 2: Sampling criteria for tube and block samplers (NNI, 2018).

Column	1	2	3	4	5		6	7
Line	Type of sampler [b]	Preferred sample dimensions — Diameter mm	Length mm	Technique used	Applications and limitations — Unsuitable for	Recommended for use in		Sampling category for soils as in column 6 [a]
1	thin-walled (OS-T/W)	70 to 120	250 to 1000	static or dynamic driving	gravel, loose sand below water surface, firm fine soils, soils including coarse particles	fine or organic soils of soft or stiff consistency		A
						(medium) dense sand below water surface		C (B)
						fine or organic soils of stiff consistency		B (A)
2	thick-walled (OS-TK/W)	>100	250 to 1000	dynamic driving	gravel, sand below water surface, pasty and firm fine or organic soils, soils including coarse particles	fine or organic soils of soft to stiff consistency, and including coarse particles		C (B)
3	thin-walled (PS-T/W)	50 to 100	600 to 800	static driving	gravel, very loose and dense sands, semi-firm and firm fine or organic soils, soils including coarse particles	fine or organic soils of pasty or stiff consistency, and sensitive soils		A
						sand above ground water		C
4	thick-walled (PS-TK/W)	50 to 100	600 to 1000	static driving	gravel, sand below water surface, pasty and firm fine or organic soils, soils including coarse particles	fine or organic soils of soft to stiff consistency, and sensitive soils		B (A)
5	cylinder (LS)	250	350	static rotating	sand	clay, silt		A
6	cylinder (S-SPT)	35	450	dynamic driving	coarse gravel, blocks	sand, silt, clays		D
7	window	44 to 98	1500 or 3000	static or dynamic driving	sand, gravel	silt, clay		D (C)

[a] If the sampling categories given in brackets are used in particular favourable ground conditions – which shall be explained in such cases – the higher quality classes indicated in the brackets can be achieved.

OS-T/W open-tube samplers, thin-walled	PS-TK/W Piston samplers thick-walled
OS-TK/W open-tube samplers, thick-walled	LS Large sampler
PS-T/W Piston samplers thin-walled	S-SPT SPT sampler

The ASTM standard for the 'Selection of Soil and Rock Sampling Devices Used With Drill Rigs for Environmental Investigations', ASTM D6169 (2005) gives guidelines for appropriate sampling practice of soils. Table 3 shows criteria for suitability of material sampled grouped by different types of samplers. Both the ISO-22475 (2018) and ASTM D6169 (2005) standards acknowledge the same sample qualities are achieved by sampler type, however differences in nomenclature feature between the two. For example, according to the ISO standard (NNI, 2018), a thin-walled sampler will achieve a category A sample (highest possible category) for fine and soft or stiff soils and the ASTM standard describes fine grained soft or stiff soil samples from a thin-walled sampler as E (Excellent, highest possible category).

Table 3: Suitability of core sampling devices for different geologic materials (ASTM D6169)

Sampler Type	Soil/Unconsolidated Material[B]					
	Fine-Grained		Coarse, Cohesive		Cohesionless[D]	
	Soft-Stiff	Stiff-Hard	Sand	Gravel	Loose	Dense
Drive/Push Samplers						
Thick-Wall	E-G	G-P	E-G	F-P	F-P	G-P
Thin-Wall	E	F-P	G-F	NA	F-P	P
Piston[E]	E	F-P	G-F	NA	E-P	P
Rotating Soil Core Samplers						
Hollow-Stem Auger	G-F	E-G	E-G	F-P	F-P	G-P
Pitcher	G-F	E-G	E-G	G-P	G-P	E-P
Denison[F]	G-F	E-G	E-G	G-P	F-P	G-P

Ratings: E = excellent; G = good; F = fair; P = poor; NA = not applicable.

D Loose cohesionless soils are difficult to recover with most drive/push sampling devices unless retainers are used, especially when saturated. Materials in this category include saturated sensitive clays, silts and sands, sensitive organic silts, soft clays, unsaturated loose sands and silty sands. Very dense soil material is also difficult to penetrate with most drive/push sampling devices. Examples of dense materials would include compact tills and weakly cemented soil/rock.

E Numerous types of piston samplers have been developed, but only a few are commercially available; many are effective in sampling saturated, cohesive soils, but have varying effectiveness for sampling cohesionless soils. F Denison sampler ratings are for soil sampling

configuration with inner barrel advanced ahead of outer rotating core barrel. In the rock coring configuration ratings are same as for double tube RBD sampler.

3.4 Indices and methods used to indicate degree of disturbance

A wide range of indices and methods have been used to estimate sample disturbance. However, certain conditions, such as OCR, soil type and plasticity index, need to be met for every index and method. Amundsen et al. (2015) summarizes some indices and methods in Table 4. Regarding peats, no proven sample disturbance index/method currently exists.

Table 4: Indices and methods of quantifying sample disturbance (Amundsen et al., 2015).

Year	Method	Para-meter	"Very good to excellent" quality	"Very poor" quality
Triaxial and oedometer tests:				
1979-1988	Volumetric strain (ε_{v0}) at *in situ* effective stress (σ_{v0}') (Andresen and Kolstad, 1979), (Lacasse and Berre, 1988)	ε_{v0}	<1%	>10%
1996	Specimen Quality Designation (SQD) (Terzaghi et al., 1996)	ε_{v0}	<1%	>8%
1997	Change in void ratio ($\Delta e/e_0$) (Lunne et al., 1997), which depends on the overconsolidation ratio (OCR)	$\Delta e/e_0$	<0.04(OCR 1-2) <0.03(OCR 2-4)	>0.14 OCR 1-2) >0.10(OCR 2-4)
2013	Oedometer stiffness ratio (Karlsrud and Hernandez-Martinez, 2013)	M_0/M_L	>2.0	<1.0
Uniaxial compression tests:				
1979	Strain at failure (ε_{vf}) in an unconsolidated and undrained (UU) test on soft clay (Andresen and Kolstad, 1979)	ε_{vf} (UU)	3-5%	10%
1980	Unconsolidated and undrained shear strength, s_u (UU), measured in the laboratory (Ladd et al., 1980), (Ladd and DeGroot, 2003)	s_u (UU)	Relative assessment based on information about stress history and predicted strength using SHANSEP	
Suction and shear wave velocity measurements:				
1963-2002	Residual effective stress (σ_s') and the effective stress for a "perfect sample" (σ_{ps}') (Ladd and Lambe, 1963), (Hight et al., 1992), (Ladd and DeGroot, 2003)	σ_s'/σ_{ps}'	≈0.25-0.50 (OCR>1.5) ≈0.05-0.25 (OCR<1.5)	
1996-2000	Soil suction (u_r) (Tanaka et al., 1996), (Tanaka, 2000)	u_r/σ_{v0}'	≈ 1/5 to 1/6	
2007	Shear wave velocity (V) (Landon et al., 2007), V_{vh} is measured in the field and V_{SCPTU} is from SCPTU.	V_{vh}/V_{SCPTU}	≥0.60	<0.35
2010	Combination of normalized shear wave velocity (L_{vs}) and normalized soil suction (L_u) (Donohue and Long, 2010)	L_{vs} L_u	L_{vs} < 0.65 L_u < 0.4	L_{vs} > 0.8 L_u > 0.6
1985-2014	Radiography (Ladd and DeGroot, 2003)	Visual identification of sample disturbance.		

The strain experienced to load a specimen back to in-situ effective stress is expressed by ε_{v0}. A sample quality criterion was proposed by Andresen and Kolstad (1979) based on shallow onshore clay shown in Table 5. Excellent sample quality is akin to a ε_{v0} of less than 1, indicating negligible disturbance. It is questionable if this criterion can be applied to peats. Furthermore, it was proclaimed by Lacasse and Berre (1988) that this criterion was too conservative for the intended onshore clays. The reason this is questionable to apply to peats is because a change in pore volume has a greater effect to the skeleton structure, the lower the initial pore volume of the sample, thus causing sample disturbance. Therefore, this criterion may be applied to soft plastic clays, but likely not reliably to peats.

Table 5: Oedometer sample quality criteria (Andresen and Kolstad, 1979).

Sample Class	ε_{v0} (%)	Sample Quality
1+	< 1	Excellent
1	1 – 2	Very Good to Excellent
2	2 - 4	Good to Fair
3	4 – 10	Poor
4	> 10	Very Poor

In order to quantify sample disturbance, Lunne et al. (1997) proposed to use the disturbance index, represented by the Δe, when consolidated back to in-situ effective stresses during the triaxial, direct simple shear (DSS) or oedometer test, divided by the initial void ratio (e_0) denoted by $\Delta e/e_0$. Table 6 shows the categorization of quality types ranging from "Excellent" to "very poor" (Lunne et al., 1997). Previously, the change in volumetric strain (ε_{v0}) at in-situ vertical effective stress (σ_{v0}') was used to measure sample disturbance (Andresen and Kolstad (1979), Lacasse and Berre (1988)). It must be noted, that this disturbance criteria (by Lunne et al., 1997) was based on tests carried out on marine clay samples with properties: plasticity index 6%–43%, w 20%–67%, OCR 1–4, and depth 0–25 m below ground level. Therefore, the soils to be investigated in this thesis (organic clays and peats) should fall within these ranges so that the $\Delta e/e_0$ may be used with confidence. However, peat will certainly have a much higher w than the maximum range stated. Alternatively, the oedometer stiffness ratio, M_0/M_L, by Karlsrud and Hernandez-Martinez (2014) may be used to model disturbance, which relies on the maximum constrained modulus in the overconsolidated stress range (M_0) and the minimum constrained modulus after preconsolidation stress (M_L). When disturbance increases with this measure, it signifies a denser soil structure caused by volumetric changes during reloading.

Table 6: Proposed criteria for evaluation of sample disturbance by Lunne et al. (1997).

OCR	$\Delta e/e_0$			
	Very good to excellent	Good to fair	Poor	Very poor
1-2	<0.04	0.04-0.07	0.07-0.14	>0.14
2-4	<0.03	0.03-0.05	0.05-0.10	>0.10

Landon et al. (2007) used the bender element test to measure resulting shear wave velocities (V_s) in soft clays. In order to quantify the disturbance, the V_s of the sample was measured immediately after the sampling procedure in the field (V_{vh}) and compared to the shear wave velocity of the soil before sampling (V_{SCPTU}) with the use of a Seismic Cone Penetration Test (SCPTU) (Landon et al., 2007). The established disturbance index based $\Delta e/e_0$ was compared to the differences in shear wave velocity, shown in Figure 17. Samples are rated based on the following criteria: Very Good to Excellent and Fair to Good Quality: $V_{vh}/V_{SCPTU} \geq 0.60$. Poor Quality: $0.35 \leq V_{vh}/V_{SCPTU} < 0.60$. Very Poor Quality: $V_{vh}/V_{SCPTU} < 0.35$ (Landon et al,. 2007). In order to validate the use of the shear wave velocities to quantify sample disturbance, V_{vh}/V_{SCPTU} was plotted against $\Delta e/e_0$, showing a linear trend (Figure 17(c)). In accordance with the $\Delta e/e_0$, shear wave velocities show that less disturbance is caused by sampling with the Sherbrooke block sampler than with the piston samplers. It was concluded that bender element testing serves as a non-destructive, rapid and portable method to determine sample disturbance (Landon et al., 2007).
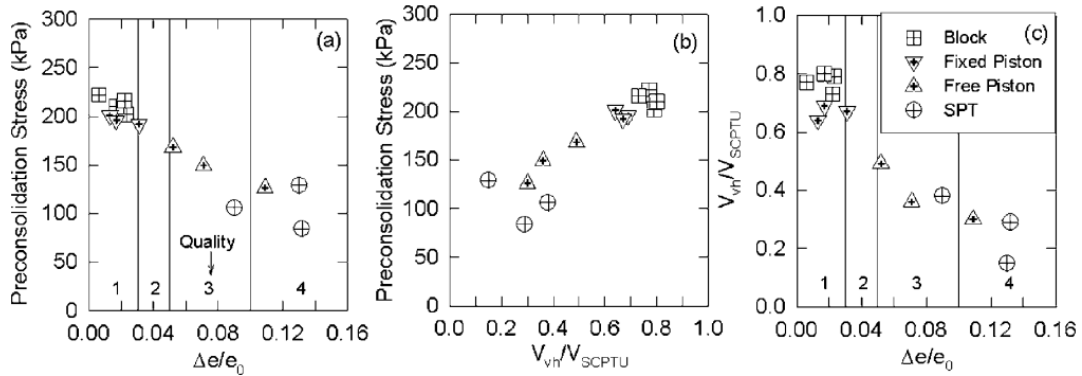
Figure 17. Comparisons of different sample disturbance parameters (Landon et al., 2007).

3.5 Using CT scans as a measure of sample disturbance

CT scanning is described by Ladd and DeGroot (2003) as a very cost effective method because it enables the separation of poor quality samples from sufficiently undisturbed samples without opening the container. This is especially important in expensive sampling operations such as offshore sampling or onshore sampling when costly samplers such as the Sherbrooke block sampler or DLDS are involved. The degree and nature of sample disturbance via CT scanning can be measured by the following identification features: bending near the tube perimeter, cracks due to stress relief (e.g. gas exsolution) and voids due to sampling disturbance, often near the ends of the tube. In a paper investigating the damage caused to archaeological structures by one-dimensional loading, Ngan-Tillard et al (2016) observed the structural changes in peat and organic clays with micro-CT scans. As shown in Figure 18, the fibres have compacted together with the surrounding soil matrix compared to the sample before one-dimensional loading. However, it is unclear whether and how the orientation of the fibres changed. CT scanning is most efficient in mediums with contrasting density distribution, however, due to the high w usually encountered in peat, it may lead to insufficient density contrast in images.
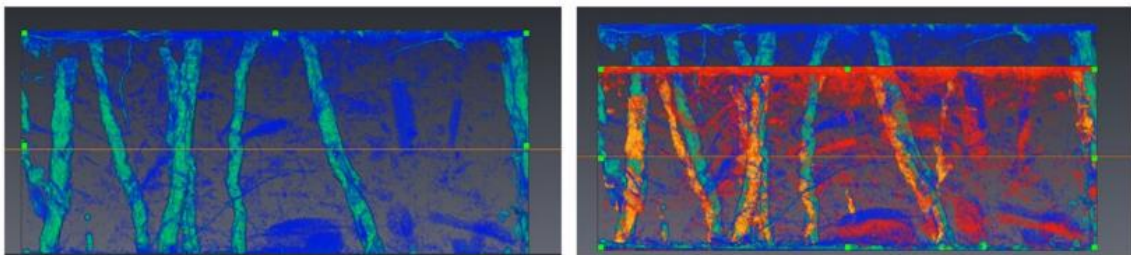
Figure 18. Micro-CT scans of subvertical rootlets and other plant matter in a 50 mm oedometer sample, (left) before loading (in blue) and (right) after loading (in red) which underwent a maximum pressure of 180 kPa (Ngan-Tillard, 2016).

4 Methodology, data gathering and processing

The methodology, data gathering and processing section describes the approaches used to acquire the data necessary to formulate conclusions based on the research questions. Data collection methods were carried out in parallel, due to the time-intensive nature of organizing and performing certain methods such as the IL oedometer tests and STOWA database collection. In Table 7, the test type(s) conducted for each sample and specimen of the SDT database are highlighted.

Table 7: Constituents of SDT database.

Sample name	Specimen name [1]	IL Oedometer test	Pycnometer test	Bender element test	Medical-CT scan [2]	Micro-CT scan MR [3]	Micro-CT scan HR [4]	Sieve test
VN75740-2-2A	A1	√	√					
	A2	√	√					
VN75740-2-2C	A3	√	√					
	A4	√	√			√√ [5]	√√ [5]	
11204108	D1	√	√		√			
	D2	√	√					
VN80625-1-1	D3	√	√					√
	D4	√	√			√√ [5]	√√ [5]	
VN80625-1-2	D5			√				
	D6			√				
	D7			√				
VN80625-1-3	A5			√				
VN75740-3	-				√			
VN75740-5	-				√ [6]			

[1] A = Ackerman sampler, D = DLDS

[2] With x and y resolution of 0.3 mm and z (horizontal) resolution of 0.6 mm. Scans were made on the whole block or tube sample.

[3] Medium Resolution: 23 microns.

[4] High Resolution: 5 microns.

[5] Indicates two scans were performed, one before and one after the 1D compression test.

[6] Two scans performed, one without removing sample from the Ackerman tube, one after removal from tube.

The methods and apparatus used in this investigation encompass a wide range of length scales, as demonstrated by the order within Figure 19. In the figure, the lower boundary next to the stated method indicates the order of magnitude of the highest resolution for said method. Meanwhile, the upper boundary is the maximal measurement scale at which the method may be applied. For example, the micro-CT has a maximum resolution of 5 microns (10^{-6} magnitude) and the measurements are applied over whole specimens which are restricted to the size of a few centimetres in any of the axes (10^{-2} magnitude).
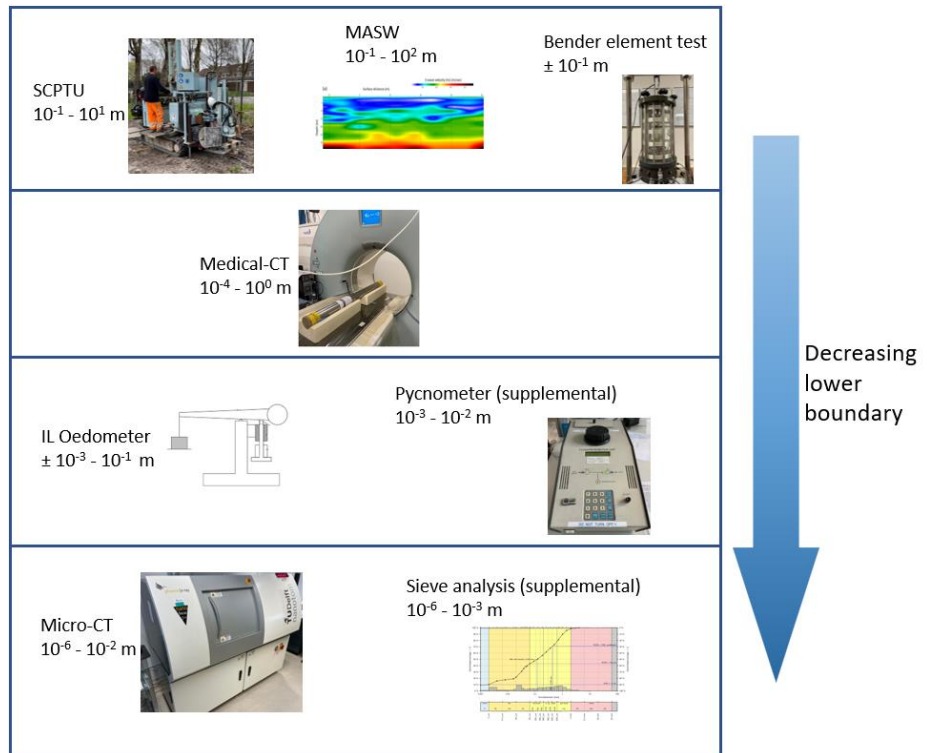
Figure 19. Scales of measurements and resolutions.

4.1 Radiography

4.1.1 Medical-CT scans

Medical-CT scans are efficient in scanning large soil masses quickly to identify disturbance features such as bending near the tube perimeter and density changes within the sample. Therefore, an appropriate use for this technique is for qualitative analysis of samples, as quantitative analysis may lead to significant errors due to the much lower resolution compared to the micro-CT scanner. The resolution for the scans were 0.6 mm in the z axis, which is in the length direction of the tube, and 0.3 mm in the x and y axes, perpendicular to the tube length, with a scanning kilovoltage of 140 (kV). Figure 20 shows the medical-CT scanner of TU Delft used for scanning the block sample and Ackerman sample before and after extraction from the tube. The resulting greyvalue intensity of the medical-CT scan has Hounsfield units (HU) due to the calibration ability of the device. Images were preserved at 64-bit to maintain resolution. On the HU scale, a value of -1000 represents air and 0 represents water. The range of HU for these images was from -1024 to 2844.
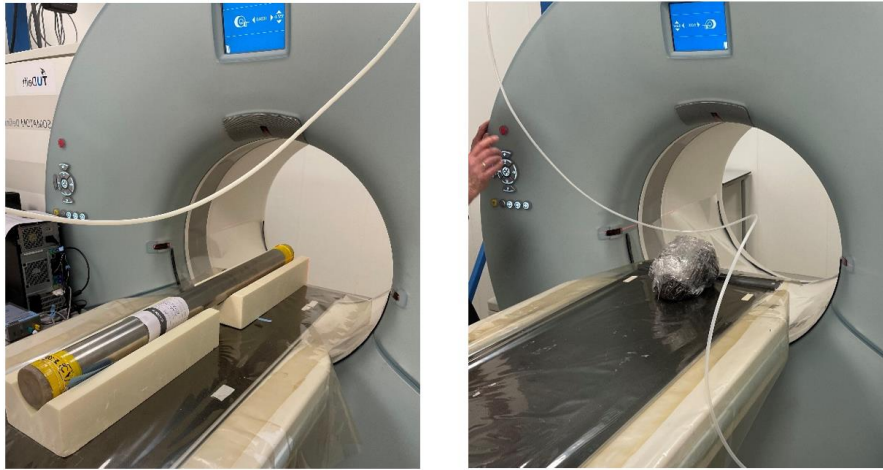
Figure 20. Medical-CT scanning of peat in Ackerman tube (left) and peat DLDS block (right).

Beam hardening is encountered in CT scanning when the edges of an object return a higher greyvalue intensity than the centre of the specimen, even if the material has the same density throughout. This is due to the differences in penetration of the spectrum of X-ray energy delivered by the CT scanner, especially when highly dense materials in the CT cell absorb the photons before reaching the intended material for scanning. In this investigation, this was mitigated for micro-CT scans by housing all samples in plastic wrapping sheet, which ensures moisture retention as well. For medical-CT scans, beam hardening correction was needed for the scan of the peat sample within the steel Ackerman tube, due to the high density stainless steel absorbing excess amount of photons. While beam hardening correction by the built-in medical-CT scanner software greatly reduced the effect, as Figure 31 in section 5.1.1 shows, beam hardening is still present close to the tube wall. The scans were analysed with the use of the image analysis program Fiji, also named ImageJ.

4.1.2 Micro-CT scans

Micro-CT scans were performed on samples before and after consolidation using a Nanotom NF180 x-ray CT scanner at TU Delft (Figure 21). Due to the high variability in grain size of peats, scans of samples with a resolution of 5 μm were made in addition to the standard resolution of 23 μm for this investigation. In order to validate the resolution used for micro-CT scanning, a wet-sieve analysis was conducted on the same peat subject to IL oedometer testing and scanning, to determine a grain size distribution. The highest permissible resolution being determined by the diameter of the specimen, resulted in a diameter of 11 mm and 65 mm being used, for the 5 μm and 23 μm resolution scans respectively. The resulting micro-CT scan greyvalue intensities are uncalibrated, due to the machine lacking the function to do this. This is due to differences in machine requirements between the micro-CT scanner and the medical-CT scanner, whereby all medical-CT scans must adhere to calibration to real life density and micro-CT scanners must not. The scans could then possibly be manually calibrated to reference objects in the scan of known density such as air and sand grains. Likewise to the medical-CT scan, images were preserved at 64-bit images.

Figure 21. Nanotom TU Delft micro-CT scanner.

The following summarized procedure was carried out for all micro-CT scans of 23 μm resolution detailed in Table 7. As with the medical-CT scans, the micro-CT scans were analysed with Fiji. Greyvalue thresholds were used to binarize air-filled pore space and silica grains, in order to isolate the peat and water in the scans. A Z Projection was made for the mean greyvalue intensity and standard deviation of the column. Following this, 200 concentric circles were created on both Z Projections, for which the average greyvalue intensity and standard deviation along the perimeter of each circle was calculated as shown in Figure 22. This enabled the creation of a greyvalue intensity vs radius graph, which is a proxy measure for sampling densification with increasing radius, with the aforementioned standard deviation measure used to calculate the standard error at each of the 200 radii. The methodology used within Fiji is presented in Appendix D with greater detail.
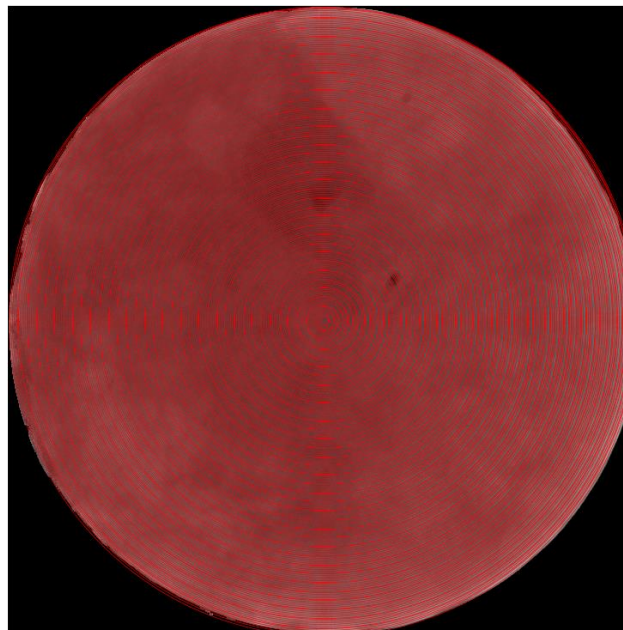
Figure 22. Concentric circles in Fiji.

4.2   SCPTU, MASW and Bender element tests

In order to measure the in-situ V_{SCPTU}, seismic cone penetration tests (SCPTU) were deployed in Gouda (Figure 23) using both the Geomil and APvdBerg acquisition systems. Two batting beams, each fitted with two sledgehammers of 10 kg) were placed at 2 m and 5 m from the cone of the CPT rig in order to provide the necessary seismic wave. A minimum of three readings were taken per beam, per interval of 0.5 m, until the sand layer at -11 m NAP was reached. For this location, the soil layer interpretation from previous CPT tests were: Topsoil from NAP -2.5 m to NAP -3.5 m, followed by clay until NAP -4 m, peat till NAP -8 m and organic clay until the sand layer at -11 m NAP. Unfortunately, the APvdBerg system had a fatal equipment failure upon reaching the NAP -5.0 to -5.5 m interval, therefore, no data was recorded with this system lower than this depth.

Figure 23. CPT rig with SCPTU modifications.

As a mean to validate the SCPTU tests, Multichannel Analysis of Surface Waves (MASW) were carried out at the same site in Gouda, as displayed in Figure 24. The shear wave velocities resulting from this method were compared to the shear wave velocities from the SCPTU tests. In this array, 48 vertical 4.5 Hz geophones were spaced at one metre from one another. The geophones used in this operation had a distortion of less than 0.3% for the measured shear wave velocities in the raw seismograph. The reading interval was conducted from a mobile source every six metres, parallel to the geophone array. Similarly, the SCPTU set-ups utilized a sledgehammer of 10 kg as the source of seismic waves, with five seismic input signals made per interval to constitute an average.

Figure 24. Multichannel analysis of surface waves (MASW) at the site in Gouda.

Before conducting the bender element tests, samples were first saturated to a B-value of at least 0.97, which is used to evaluate the degree of saturation of the specimen. Subsequently, they were consolidated back to its in-situ σ_v within a conventional triaxial rig, at the laboratory of geotechnical firm Wiertsema & Partners (Figure 25). The height and diameter of the samples before consolidation were 10 cm and 5 cm, respectively. An input wave with a period of 0.2 ms and a voltage of 14 V was used to induce the resulting output wave during the bender element tests. The peak-to-peak method was used in order to determine the V_s, which entails measurement of the time difference between the transmitted peak and the received peak. An average V_s per specimen was produced based on 10 V_s measurements.

Figure 25. Bender element set-up within triaxial rig.

4.3 IL oedometer tests

In addition to consolidation data collection from databases, different tests were carried out on newly sampled Ackerman and DLDS peat and organic clay samples for this study, from sites in Vlist and Gouda, which formed part of the SDT database. The IL oedometer test for this investigation had to follow the same procedure as used in the STOWA's database oedometer results in order to minimize bias in the methodology. These IL oedometer guidelines in STOWA's database come from the Dutch 'Macro Stability Schematic Guide' (Ministry of Infrastructure and Water Management, 2016). Firstly, the volumetric weight of the sample was determined by measurement of the soil mass and volume of the sample, followed by calculation of the in-situ σ_v'. After determination of the in-situ σ_v' the sample was subject to, specific loading steps were used depending on the calculated in-situ σ_v', in conform with Table 8. As shown in Figure 26, the IL oedometer was connected to a displacement transducer (and computer), which allows for continuous measurements, with a reading interval of 10 seconds.

Table 8: Stresses per loading step, standardized to the σ_v' (Ministry of Infrastructure and Water Management, 2016).

σ'_{vi} [kPa]	Loading step								
	1	2	3	4	5	6	7	8	9
<50	0.25	0.5	1	2	4	2	4	8	16
>50	0.25	0.5	1	2	4	2	4	10	

From each sample, two specimens were prepared with varying specimen height of 19.5 mm and 29.5 mm. Specimens from Ackerman samples were cut from the mid-point of the tube height, using a sharp knife for peats and a wire saw for organic clays. The Ackerman specimens underwent negligible additional disturbance during the cutting procedure with the cutting ring, due to the near identical inner diameter of ~65 mm used for both devices.

Figure 26. Incremental loading oedometer cell used to consolidate samples at TU Delft.

After completion of the last loading step, the data was processed using methods from the Dutch guidelines for oedometer test execution and interpretation (CUR, 2005). Firstly, for each specimen, the time needed to reach 100% primary consolidation (t_{100}) for each loading step was found with the use of

the Casagrande and Taylor methods, which is needed in order to calculate the strain and e, as shown in Figure 27. The intersection point between the tangent of the inflection point of the load step and the tangent of the straight portion of the lower part of the curve. This was often non-trivial and subject to bias, due to the nature of the high compressibility of peat settlement, which causes the interface between primary and secondary consolidation to be difficultly recognizable. In order to add certainty to this measurement, the alternative Taylor $\sqrt{t}$ – method was used. Occasionally, the difference in t_{100} values between the Casagrande and Taylor methods was one order of magnitude. The effect of this is further discussed in section 5.3.1. Then, as presented in Figure 28, the Casagrande method was used to find the pre-consolidation pressure, which is necessary to calculate the OCR. The pre-consolidation pressure with this method is indicated by the intersection point of the bisector line of the tangent at the point of highest curvature with the tangent line of the curve after the recompression step. Subsequently, the *RR* was derived, which is defined by equation 2, calculated between loading step 6 and 7.

$$RR = \frac{\Delta \varepsilon}{\Delta \log(\sigma'_v)} \tag{2}$$
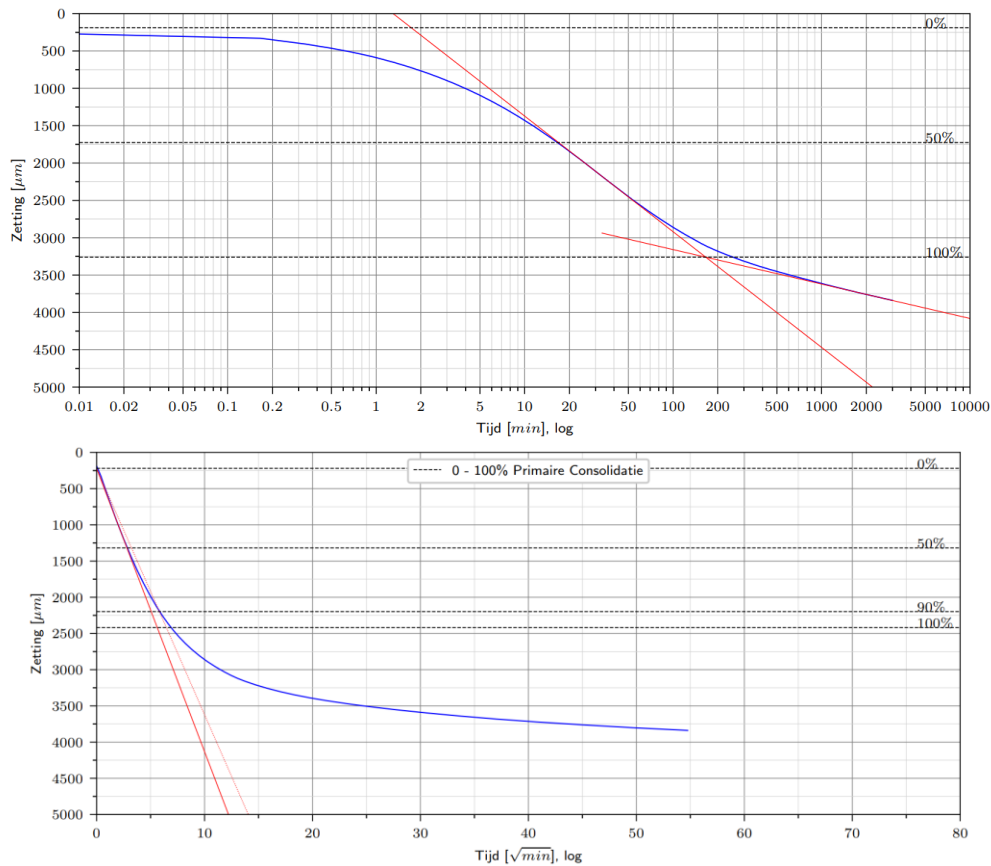
Figure 27. Settlement graphs of peat sample A4, loading step 8 on a Casagrande semi-log time scale (top) and Taylor square-root time scale (bottom) to find the t100).
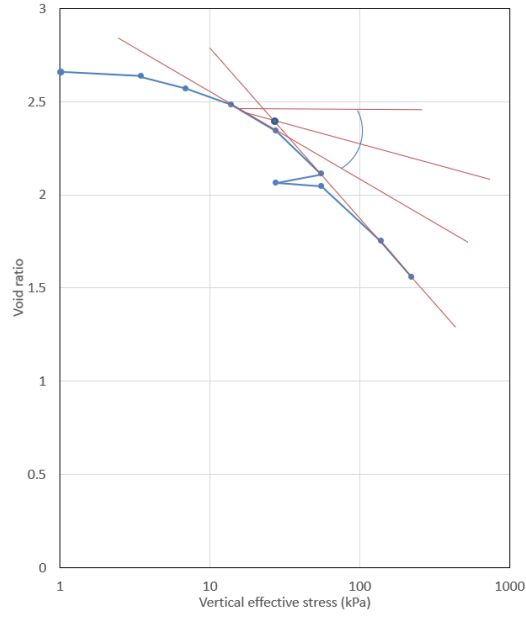
Figure 28. Casagrande method to find pre-consolidation pressure of the sample A4.

4.4 Pycnometer test, oven-dry method and wet-sieve analysis

In order to determine the specific gravity, also known as relative density (G) and dry volumetric weight (γ_d), the pycnometer test and oven-dry method were carried out respectively. These tests enabled the use of equation 3 to determine the e_0, used to produce the $\Delta e/e_0$. The helium gas-based Ultrapycnometer 1000 device (Figure 29) was used on dried soil, which had been dried in an oven at 70°C for at least 24 hours. Then, the soil was weighed and subsequently placed in the container of the device and ten volume measurement runs were carried out per specimen by the device. Similarly, the oven-dry method was used at 70°C for at least 24 hours, at a known prior volume, then weighing the soil, followed by the use of equation 4 to determine the dry volumetric weight. The temperature of 70°C was used for the prolonged period of time in order to not risk combustion of the organic material in the samples. Sample weighing had to be done swiftly as to avoid an increase in sample weight as the peat absorbs humidity from the surrounding air.

$$e_0 = \frac{G*\gamma_w - \gamma_d}{\gamma_d} \tag{3}$$

$$\gamma_d = \frac{W_d}{V} \tag{4}$$

Figure 29. Ultrapycnometer 1000 device.

A wet-sieve analysis was performed on peat, with the aim of creating a grain size distribution and providing an indication of the resolution needed for CT scanning. This analysis was conducted with the auto-analyser at the laboratory of Wiertsema & Partners on sample VN80625-1-1.

4.5   DLDS and STOWA Database

Since only one DLDS rig exists, which has been operational since 2017, the available data is limited. Additionally, the data needs to be applicable to this thesis, whereby a IL oedometer tests needs to have been carried out. The same set of geotechnical parameters were filtered from the DLDS database as from the STOWA database.

In the Netherlands, regional waterboards contract geotechnical sampling companies to collect geotechnical data and store it in STOWA databases. For this investigation, waterboards of the Netherlands were approached to provide access to these databases. If it was not possible to establish contact with a waterboard representative, the database was received directly from the geotechnical sampling company involved in this thesis, Wiertsema & Partners, however, in these cases the data was anonymised to protect the contract laws between said organizations.

First of all, rows not including any IL oedometer data were filtered out, followed by the filtering of rows which did not include the appropriate soil types for this investigation. Secondly, all forms of peat classified soil data was retained, in addition to organic clays, which had humousity as a secondary soil fraction, ranging from weakly organic (h1) to very strongly organic (h4), according to the standard NEN5104 (NEN, 1989). This antiquated standard was used because the STOWA database has accumulated data based on NEN5104 (NEN, 1989) for the past decades. In order to produce the $\Delta e/e_0$ parameter by Lunne et al. (1997), the necessary Δe to in-situ σ_v was extracted from original PDF files (containing consolidation graphs and supplementary data) used to fill in the parameters of the STOWA database. Thirdly, the OCR had to be computed, as necessary for the clays tested by Lunne et al. (1997). For this, the original PDF files were again investigated, since the pre-consolidation stress had to be interpreted from the graphs showing σ_v' against strain. Lastly, the $\Delta e/e_0$ was computed and relationships between the parameters within Figure 2 were investigated.

5 Data analysis and results

This section explains how the data was analysed and the subsequent results were obtained. This section is subdivided into the methods used for soil disturbance characterization. A summary of test types performed on each sample and specimen is presented in Table 7.

5.1 Non-destructive disturbance determination methods

5.1.1 Medical-CT scans

Both quantitative and qualitative analyses were performed on the CT scans. Due to peat often falling in the same density range as water, it was difficult to distinguish between the two different mediums during image analysis in both medical- and micro-CT scans. Brighter greyscale shades on CT scans signify material with higher density.

Figure 30 (left) shows a cross-section of a medical-CT scan slice. Noticeably, cracks are prevalent in the upper half of the sample, with this observation also occurring throughout the remainder of the CT scan slices. This is believed to be due to a combination of the following factors: stress relief, gas exsolution and water migration. The reason these types of disturbances occur is due to the intermediary stage between removing the soil in blocks from the DLDS tube and laboratory testing, whereby the samples are wrapped in plastic and aluminium foil as described in section 2.3. In addition, while peat is a coarse material, pore water can easily migrate from the top of the block to the bottom. Due to insufficient lateral support and handling of the sample, distortion occurs at the edges of the block. A follow-up scan should be made of a full DLDS tube in order to confirm that this is only limited to the block format. When this is combined with a higher resolution scan, the same method may be applied as described in section 4.1.2 to determine the radial density differences (tube wall edge effect) as for the Ackerman sample. Numerous characteristic constituents of peat samples can be identified in Figure 30, such as a partially decomposed branch (label 'a'), silica grains (label 'b') and a macro pore (label 'c').
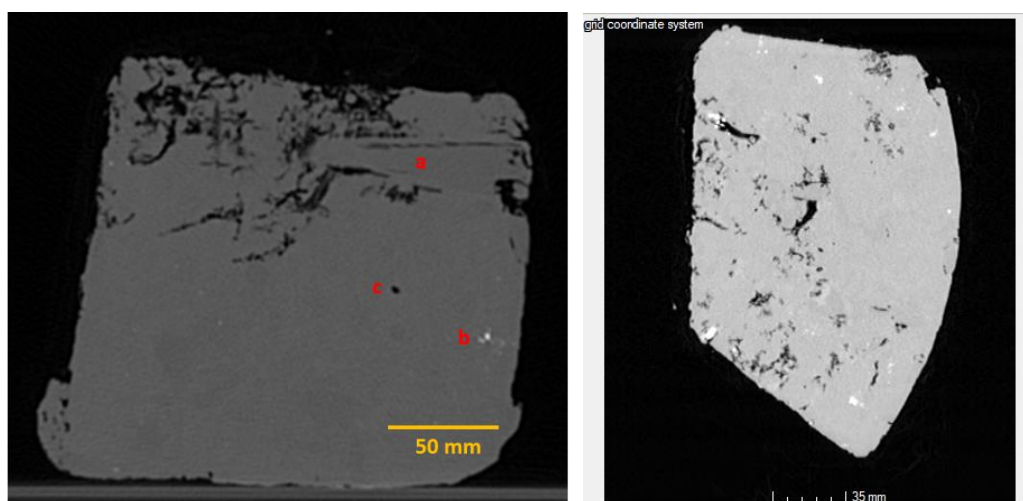
Figure 30. Cross-section (left) and top view (right) of medical-CT scan slice of peat DLDS block sample 11204108.

Scans were made before and after removing an Ackerman sample from its respective thin-walled tube. Figure 31 shows the same slice for comparison, whereby changes in structure and available pore space

can be noticed. While structure stayed the same in many slices, there were instances such as in Figure 31 which show swelling and rearrangement of structure. Using ImageJ to quantify the change in total sample volume, it was established that the total volume increase of the sample was 3.59% after extraction from the tube.
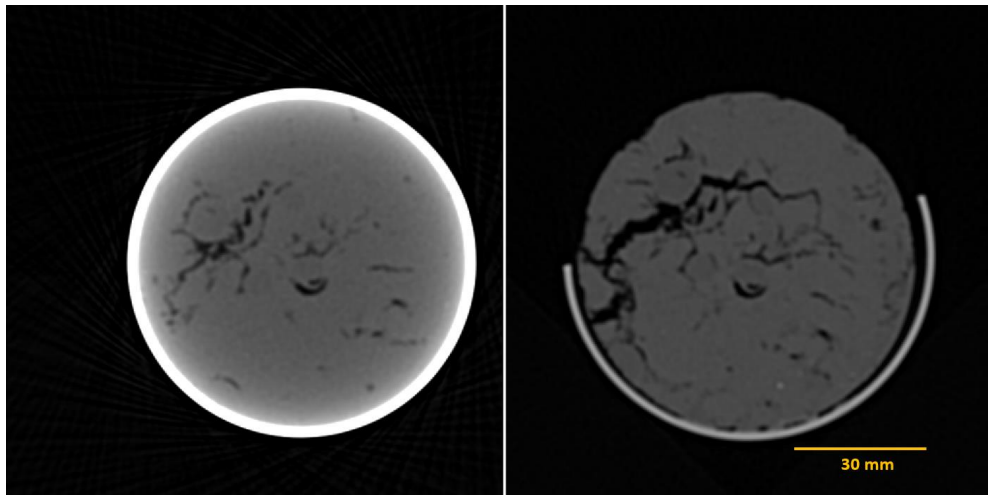
Figure 31. Top view of the same Ackerman sample before extraction from tube (left) and after extraction from tube (right).

5.1.2 Micro-CT scans

As with the medical-CT scans, several characteristic features of peat were identified in the micro-CT scan of Figure 32. Label 'a' represents a partially decomposed twig; label 'b' is silica mineral present in peat, higher density material is evident due to the white points; label 'c' shows an air-filled void; labels 'd' demonstrate regions with brighter coloured areas closer to the side walls of the Ackerman tube, indicating an increased local densification, i.e. disturbance. These scans were made with the specimens after extraction from the tube, therefore it is not possible to establish whether this slight disturbance occurred due to the extraction procedure. The wet sieve analysis conducted on sample VN80625-1-1, presented in Appendix C shows that ~24% of the grains by weight were below 23 μm of grain diameter, which is the maximum possible resolution of the micro-CT scanner for the size of these specimens.
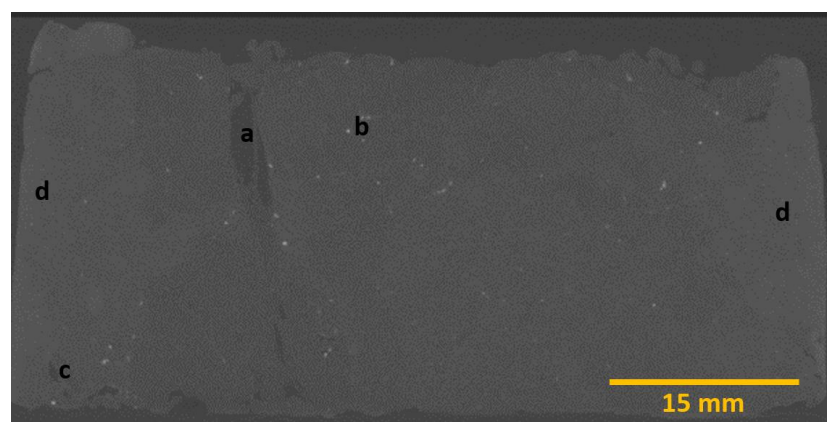
Figure 32. Cross-section of single CT scan slice of peat specimen A4 before testing.

The naming of the specimens in this section is derived by the sampling method and specimen number, i.e. 'A' stands for Ackerman specimen and 'D' for DLDS specimen. In the micro-CT scans, the

additional 'pre' and 'post' indicate whether the scan was made before or after 1D compression testing. As detailed in the procedure of section 4.1.2, concentric circles of the specimen scans in Fiji averaged the greyvalue intensity over increasing distance from the centre of the specimen. The results are plotted in Figure 33, with Table 9 showing the differences of the disturbed perimeter effect. The increase in greyvalue intensity (%) was computed from the increase of the mean greyvalue intensity over the first 37% of the radius to the peak greyvalue intensity. The 37% distance was established arbitrarily, as it was observed that after this the specimens showed a constant increase in greyvalue intensity. During 1D compression, specimen A4post experienced a maximum strain of 45.9% and specimen D4post experienced a maximum strain of 75.5%, with both specimens having a height of 29.5 mm. Naturally, these strain levels were not preserved when the samples were unloaded, the samples swelled, refilling some of the pore space with air, which has a significantly lower density than water. Due to this process, coupled with evaporation of water from the specimen until the scan could be made, is the reason that A4post has a lower greyvalue intensity profile than A4pre in Figure 33. While the greyvalue average intensity is higher after 1D compression for the DLDS sample in Figure 33, when observing the difference between the air peaks and peat peaks reported in Table 17 of Appendix D, it is evident that the difference between peaks is less for D4post, which signifies a decrease in density as with A4post. The increase in greyvalue intensity (%) is higher for the specimens after the 1D compression test when compared to the scan before 1D compression, with the Ackerman sample increasing from 10.97% to 12.28% and the DLDS from 1.49% to 1.82%, as presented in Table 9. However, this mainly demonstrates that Ackerman specimens increase radially in greyvalue intensity, more so than the DLDS specimens. Additionally, the effect of densification at the perimeter of D4pre (1.49%) and D4post (1.82%) may be caused by sample preparation with the oedometer cutting ring, which the Ackerman samples may have also been subject to, in addition to the tube wall densification.

A disadvantage from the micro-CT scans is that specimens A4post and D4post were left uncompressed for several days after completing their respective IL oedometer test, before the CT scan took place. As previously mentioned, this caused swelling, which means that these results underestimate the density difference as a function of distance to the centre of the specimen that would be experienced under natural conditions. However, this was necessary, as a micro-CT scan at the required resolution takes more than one hour to scan and reconstruct, and a large rate of swelling is not permissible during the scanning as the image might be distorted due to the changing sample volume. Although difficult to observe in Figure 33, a trough is present in specimen D4pre, halfway through the total specimen radius, which is due to the presence of a vertically aligned twig as shown in Figure 34. This is an air-filled twig, which is recognized by the darker shading within it, therefore causing a decrease in greyvalue intensity. Higher density soil encountered towards the wall of the consolidation cell during 1D compression testing, regardless of sampling method used, is due to the friction between the wall and the soil as detailed by van Essen (2021). In the paper, it is suggested to decrease the load value used in calculations of IL oedometer tests by 7% for specimens of diameter 63 mm. This is due to the load not being fully transferred to the sample, therefore the true load on the sample is less than the load applied. The friction may create abrasion, which will in turn cause a breakdown of fibres and grains in the peat at the interface between the wall and the sample, thus causing a higher density in this zone. In future studies, it would be of interest to incorporate this newly established 7% reduction on the load values in the IL oedometer section of the SDT database, to observe any trend changes when compared to other parameters.
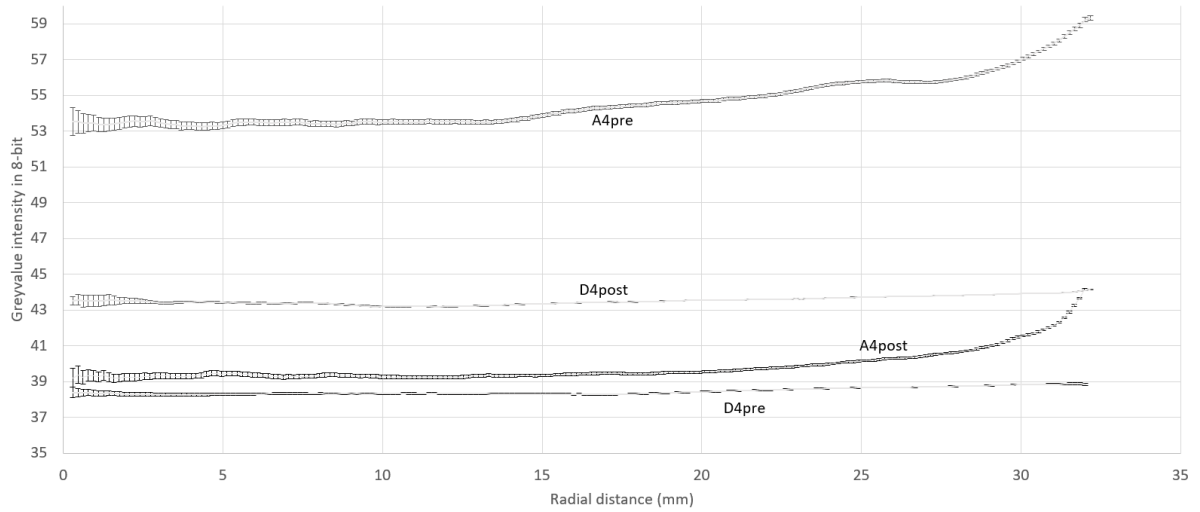
Figure 33. Radial change of greyvalue intensity in 8-bit.
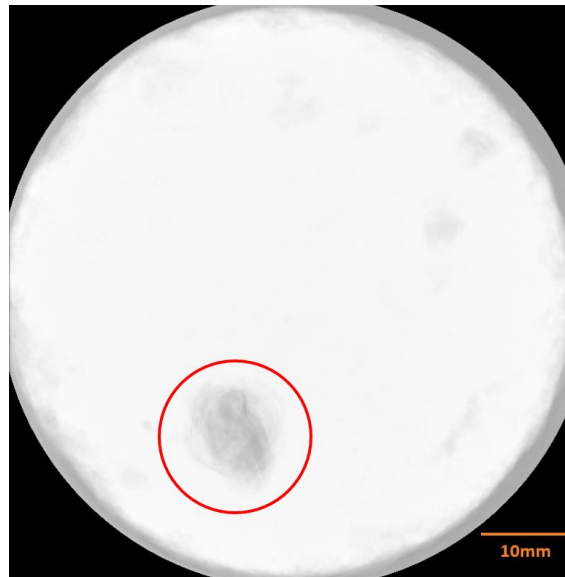
Figure 34. Top view of specimen D4pre with vertically aligned twig, shown by red circle.

Table 9: Radial densification of scanned specimens.

	A4post[2]	A4pre[3]	D4post[2]	D4pre[3]
Mean greyvalue intensity[1]	39.31	53.45	43.38	38.32
Peak greyvalue intensity	44.14	59.32	44.17	38.89
Increase in greyvalue intensity from mean to peak (%)	12.28	10.97	1.816	1.489

[1]Taken over the first 37% distance from the centre of the specimen.

[2] 'post' indicates that the scan was made after 1D consolidation.

[3] 'pre' indicates that the scan was made before 1D consolidation.

5.1.3 SCPTU, MASW and bender element tests

As shown in Figure 35, the difference in the $V_{s,b}$ between the Ackerman and DLDS techniques is considerable. At the sampling depth in Gouda, the $V_{s,b}$ of the Ackerman sample was 55.2 m/s and had a 65.4% difference to the in-situ V_{SCPTU} (28 m/s). For the DLDS sample, the $V_{s,b}$ was 48.9 m/s, equalling a difference of 54.4% to the aforementioned in-situ V_{SCPTU}. The associated standard error of the mean (SEM) [relative standard error] of the bender element test for the Ackerman and DLDS techniques are 0.12 m/s [0.23%] and 0.87 m/s [1.8%] respectively. The larger error in the DLDS is due to the fact that three samples were prepared from the same DLDS block at the same height, while only one bender element test could be done per Ackerman tube due to the diameter constraint. For the Ackerman sample, the error is based on the three output signal measurements of the singular bender element test, rather than three independent bender element tests as done with the DLDS samples. This creates an artificially lower relative standard error for the Ackerman sample, which is expected to have an error of the same magnitude as the DLDS sample, if it were possible to make multiple bender element tests from one Ackerman tube as with the DLDS block. The mean $V_{s,b}$ findings are in contrast to the results from Landon et al. (2007), due to the boundaries of the V_{vh}/V_{SCPTU} parameter in the study. In the paper, sample quality is rated based on the following criteria: Very Good to Excellent and Fair to Good Quality: $V_{vh}/V_{SCPTU} \geq 0.60$. Poor Quality: $0.35 \leq V_{vh}/V_{SCPTU} < 0.60$. Very Poor Quality: $V_{vh}/V_{SCPTU} < 0.35$. By this measurement system, the Ackerman sample $V_{vh}/V_{SCPTU} = 1.98$ and the DLDS $V_{vh}/V_{SCPTU} = 1.75$, implying that the DLDS sample is more disturbed than the Ackerman sample. The V_{vh}/V_{SCPTU} method developed by Landon et al. (2007) imply that V_s are lower in samples than in-situ. However, this is due to the fact that in the methodology described, samples were not reconsolidated back to in-situ stress, with the aim of developing a rapid method for in-field disturbance determination. The in-field bender element results were normalized to laboratory reconsolidated bender element results showing accordance in behaviour (Landon et al., 2007). If suction can be effectively applied to samples during sampling, the effective isotropic stress remains constant. In the case that suction is not applied or not applied appropriately to the sample, these in-field samples for testing will have been unloaded from their in-situ stress state and not reconsolidated, therefore the soil grains are less compacted and pore space is increased. Since shear waves are transmitted at higher velocity through soil skeleton than through voids, a decrease in V_s is the result. Therefore, a more appropriate measure for the disturbance in this study is the percentage difference between in-situ and laboratory shear wave velocities, as reported earlier in this section. Importantly, the method developed by Landon et al. (2007) was concluded to be suitable for non-organic clays only. Shear waves cannot propagate through water, while peats are known to have very high water contents. Hence, shear waves take a longer path from the seismic source to the receiver, leading to lower velocities, but more importantly a degree of error due to the unpredictable "jagged" path that may happen. This observation of decreasing shear wave velocities with increasing water content in peat was also noted by Dong (2016).
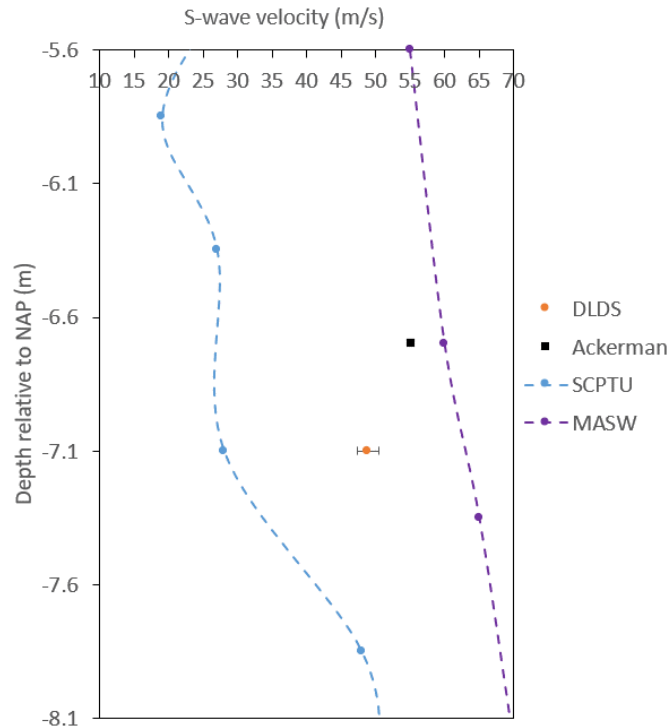
Figure 35. Shear wave velocities of DLDS and Ackerman samples with SCPTU and MASW profiles.

A source of random error for the SCPTU can be attributed to the relatively large interpolation distance because of the sampling interval of 0.5 metres. In addition, a systematic error may lie within the SCPTU Geomill system. While the distance component of the shear wave velocity measurement of the SCPTU is highly precise and accurate, the time interpretation has certain ambiguity, especially when high levels of noise are involved, as is the case with seismic analyses. The location was within 15 metres of a two way road with active car traffic, which will have had an effect on the seismic readings for both the SCPTU and MASW. However, since the signal to noise ratio decreases with increasing depth (as the wave amplitude decreases), the relatively shallow acquisition depths in this investigation are favourable. SCPTU measurements were conducted by both the Geomill and APvdBerg systems. Due to equipment failure of the APvdBerg system, only the V_{SCPTU} until the 4.5 – 5.0 m depth interval were measured, however the discrepancy between the two systems were considerable up to this depth as shown in Table 14 in Appendix B.

Due to lateral heterogeneity of soil, especially for peats, a MASW was performed at the site to validate shear wave velocities from the SCPTU. In Figure 36 (a), the spatial shear wave velocity map of the site in Gouda is shown, with the SCPTU performed at the zero mark of the horizontal distance. The coordinates from (0, 6.7) to (0, 7.1) in Figure 36 (a) is the interval of interest from where the samples were taken, for which the MASW shows a V_s of ~60 m/s. This means there is a 53.3% underestimation by the SCPTU value of 28 m/s, compared to the MASW V_s. Moreover, Figure 36 (b) shows a confidence level of ~100% in this zone, which indicates very high reliability of the modelled V_s result compared to the measured V_s. The confidence map in Figure 36 (b) is a sensitivity analysis which aids in determining how well the model fits the measurements. Moreover, the confidence level is defined by the sensitivity of the modelled dispersion curve to the V_s change at a point in the cross-section. The dispersion curve is determined in two steps, firstly a dispersion image is generated from the raw seismic field record using a wavefield transformation method, followed by extraction of the fundamental-mode dispersion curve from the dispersion image.
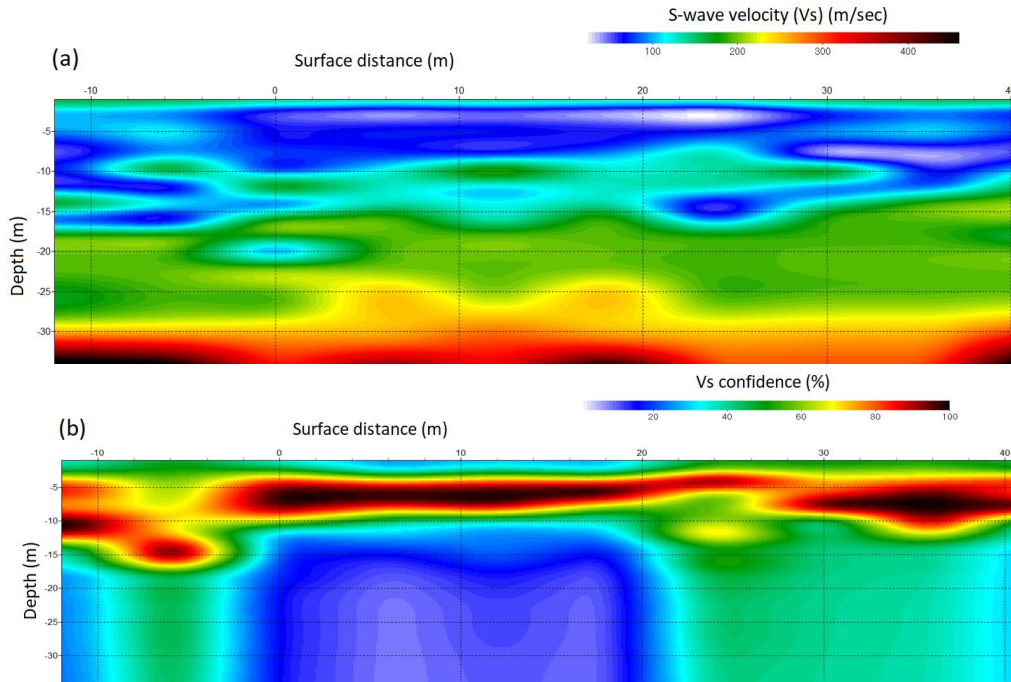
Figure 36. Shear wave velocity map as a function of surface distance and depth (1) and corresponding confidence map in % (2).

The relationship between the initial shear modulus (G_0), density (ρ) and V_s is shown in equation 5. As the V_s is squared, the G_0 is more dependent on changes in this parameter. The results show that the percentage difference between the two samplers used varies by 12.9%. At the same time, as the density between the two samplers is approximated by the increase in greyvalue intensity measures as shown in Table 9, the difference between A4pre and D4pre in this regard is 9.5%. While this does not demonstrate that the ρ and V_s must increase equally as a function of disturbance, due to methodological differences further discussed in chapter 6, it does show the implication of using an overestimated V_s for G_0.

$$G_0 = \rho * V_s^2 \tag{5}$$

5.2   1D consolidation results from databases

5.2.1 IL oedometer results from SDT Database

The general parameters for the samples from the Sample Disturbance Test (SDT) dataset, such as soil type, sampling location and depth are displayed in Table 10. The extended version of this dataset including both properties and geotechnical parameters of the dataset can be found in Appendix E.

Table 10: General information of IL oedometer tests in SDT database.

Sample name	Specimen name	Soil type	Sampling technique	Sampling location	Specimen height (mm)	Depth[1] (m)	γ_w (kN/m³)	In-situ $\sigma_v{}'$ (kPa)
11204108	D1	Peat	DLDS	Vlist	29.5	1.40	10.12	0.17
11204108	D2	Peat	DLDS	Vlist	19.5	1.40	10.12	0.17
VN75740-2-2A	A1	Organic clay	Ackerman	Vlist	29.5	2.75	15.07	13.94
VN75740-2-2A	A2	Organic clay	Ackerman	Vlist	19.5	2.78	15.07	13.94
VN75740-2-2C	A3	Peat	Ackerman	Vlist	19.5	2.50	11.08	9.70
VN75740-2-2C	A4	Peat	Ackerman	Vlist	29.5	2.53	11.08	9.70
VN80625-1-1	D3	Peat	DLDS	Gouda	19.5	5.06	9.5	41.87
VN80625-1	D4	Peat	DLDS	Gouda	29.5	5.06	9.5	41.87

[1]Depth below topsoil relative to NAP

The e_0 for the samples intended for 1D compression testing were determined from the γ_d (denoted as average density in Appendix E), computed experimentally by the pycnometer from the input mass and calculated volume. From each sample, specimens of different heights were loaded in 1D consolidation, whereby the resulting settlement was found to be proportional to the initial height of the specimen, as dictated by Terzaghi's consolidation theory.

Samples A1 and A4 are Ackerman specimens of equal dimensions but differing soil descriptions. As seen in Table 10, A1 is an organic clay specimen while A4 is a peat specimen. These were from the same site in Vlist and have comparable depths. This is of use to establish differences in consolidation behaviour and resulting consolidation parameters between organic clays and peats, which vary in organic content percentages. The stress-strain plot from the respective IL oedometer tests are shown in Figure 37. The *RR* using the Casagrande method for A1 and A4 are 0.020 and 0.030 respectively. Table 11 shows consolidation parameters processed from the SDT database. It is important to note that the $\Delta e/e_0$ was developed for use with data from CRS oedometers rather than data from the IL oedometer.

Table 11: Geotechnical parameters from SDT IL oedometer tests.

Specimen name	G	$\Delta e/e_0$ (%)	Pre-consolidation stress (kPa)	OCR	Initial volumetric w (%)	RR (Casagrande)	RR (Taylor)
D1	1.60	8.55	11.2	2.00	305	- [2]	0.056
D2	1.60	8.99	11.2	2.00	305	- [2]	0.104
A1	2.33	8.26	28.0	2.01	173	0.020	0.018
A2	2.33	7.29	32.0	2.30	173	0.016	0.014
A3	1.74	6.35	15.0	1.55	308	- [2]	0.028
A4	1.74	5.26	21.0	2.16	308	0.030	0.027
D3	1.28	35.40	20.9	- [1]	254	0.045	0.012
D4	1.28	39.40	31.5	- [1]	254	0.260	0.217

[1] The OCR for these specimens was less than 1, indicating either a strong change of the water table or a diminutive yield stress
[2] Incalculable *RR* due to erroneous t_{100} values
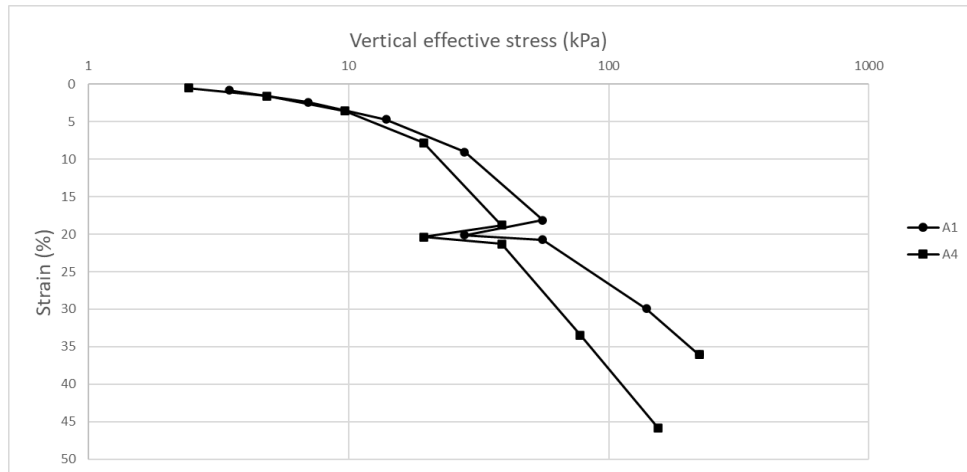
Figure 37. Stress-strain behaviour of specimens A1 and A4.

Atypical bending was observed in the void ratio to σ_v' plot for specimen D4 (Figure 38) (similarly to D3), as the curvature was insufficient to establish a pre-consolidation pressure using the methods detailed in section 4.2. A possible explanation for this result is that the yield stress is less than 10 kPa. Contrastingly, the stress on the soil might have been exceeded the yield stress due to swelling during transportation. Following this reasoning, in Table 11 the $\Delta e/e_0$ gives the impression that this is a highly disturbed specimen.
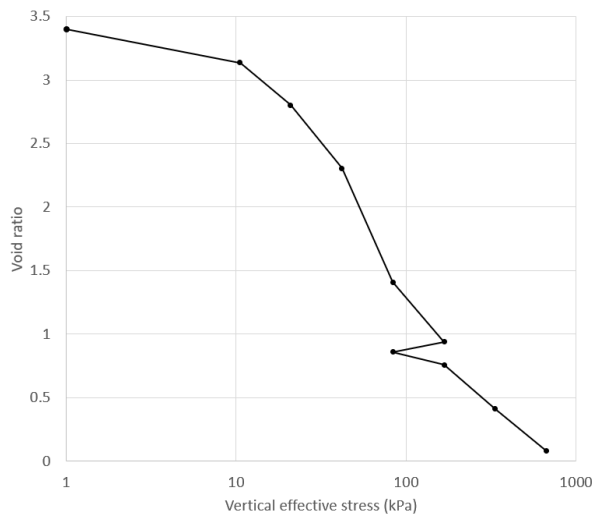
Figure 38. Void ratio vs σ_v' plot of specimen D4.

5.2.2 Summary of disturbance ratings in SDT database

The summary of quantitatively determined disturbance levels experienced by specimens forming part of the SDT database, including the non-destructive methods, are reported in Table 12.

Table 12: Summary of SDT database disturbance ratings by parameter.

Sample name	Specimen name [1]	Micro-CT scan method (%) [2]	Shear wave velocity method (%) [3]	RR (Taylor) [4]	$\Delta e/e_0$ (%) [5]
VN75740-2-2A	A1			0.018	8.26
	A2			0.014	7.29
VN75740-2-2C	A3			0.027	6.35
	A4pre	10.97		0.027	5.26
	A4post	12.28			
11204108	D1			0.056	8.55
	D2			0.103	8.99
VN80625-1-1	D3			0.012	35.40
	D4pre	1.49		0.217	39.40
	D4post	1.82			
VN80625-1-2	D5				
	D6		54.4		
	D7				
VN80625-1-3	A5		65.4		

[1] A = Ackerman sampler, D = DLDS, 'post' indicates that the scan was made after 1D consolidation, 'pre' indicates that the scan was made before 1D consolidation.

[2] Determination as shown in Table 9.

[3] Determined by the percentage difference between specimen and in-situ shear wave velocities, discussed in section 5.1.3.

[4] As determined by equation 2.

[5] Δe determined with void ratio vs stress plots, e_0 determined with the supplemental pycnometer test.

5.2.3 STOWA and DLDS databases

Typically, the $\Delta e/e_0$ is seen plotted against depth, however, in this investigation it is graphed on a $\Delta e/e_0$ vs in-situ σ_v plot, as seen in Figure 39. The range of OCR for the STOWA database was from 0.2 to 8, however, 69% of the OCR values fall within the 1 to 2 OCR range. These soils with an OCR of less than 1 indicate underconsolidation, implying that the pre-consolidation pressure is less than the σ_v'. However, the more likely cause is the inaccuracy of the yield stress used in the calculation, due to the subjectivity of observation bias, similarly to the discussed method for pre-consolidation pressure determination in section 4.3. The horizontal blue lines in Figure 39 indicate the quality boundaries as presented by Lunne et al. (1997) for clays with an OCR between 1 and 2. For this dataset, it indicates that 37% of Ackerman samples fall within the fair to excellent categories, an $\Delta e/e_0$ below 7%. All DLDS samples were under 4%, therefore ranked as "Very Good to Excellent" for sample quality. In addition, the trend is limited to the two bands seen in Figure 39, which indicate that at higher in-situ σ_v, it becomes increasingly difficult to attain Ackerman samples with an $\Delta e/e_0$ below 7%. The suitability of one parameter on another in a trend may be gauged with the use of Pearson's correlation coefficient 'r', with its mathematical expression given in equation 6. A value of 1 for Pearson's 'r' indicates a perfect linear relationship, a value of zero demonstrates no correlation and -1 shows a perfect negative correlation. While more DLDS results are needed at higher in-situ σ_v comparable to those of the Ackerman results, the $\Delta e/e_0$ vs in-situ σ_v relationship was established for the combined DLDS and STOWA databases with a Pearson's 'r' of 0.73.

$$r = \frac{\sum_{i=1}^{n}(x_i - \bar{x})(y_i - \bar{y})}{\sqrt{\sum_{i=1}^{n}(x_i - \bar{x})^2 \sum_{i=1}^{n}(y_i - \bar{y})^2}} \qquad (6)$$

With: x_i = x-variable values of dataset
$\bar{x}$ = mean of x-variable values
y_i = y-variable values of dataset
$\bar{y}$ = mean of y-variable values
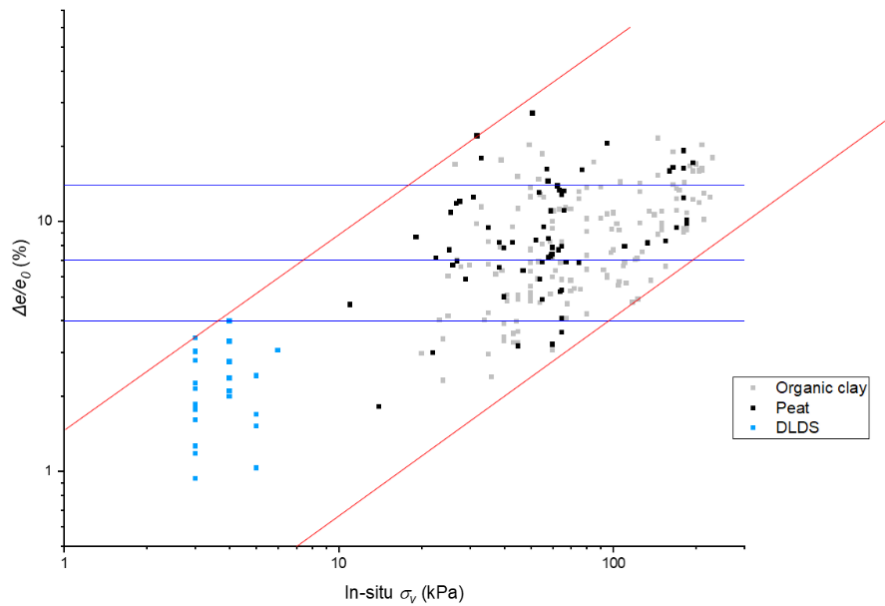
Figure 39. Logarithmic plot of Δe/e₀ vs in-situ σᵥ for STOWA and DLDS databases. The blue lines are the specimen quality levels as established by Lunne et al. (1997), with the zone below the bottom-most line described as "Very good to excellent", the next zone as "Good to fair", followed by "Poor" and the zone above the top-most line being "Very poor" quality. The parallel red lines indicate the region which the trend is observed to behave in.

The relationship explored in Figure 39 was further investigated by splitting the $\Delta e/e_0$ into its components, as shown by the plots in Figure 40. As observed, the e_0 appears to have a negative correlation with σ_v, and e_0 for DLDS peat samples are higher than for Ackerman peat samples. Meanwhile, the Δe has a random scatter for all constituents of the legend in the plot. This demonstrates that the normalization factor of the disturbance index, the e_0, biases the disturbance index when quantifying the disturbance in peats because a wide range of e_0 is possible for this type of soil, as the e_0 is influenced by the highly variable water content levels in peats, while the marine clays for which this index was developed for have a much smaller range for e_0.
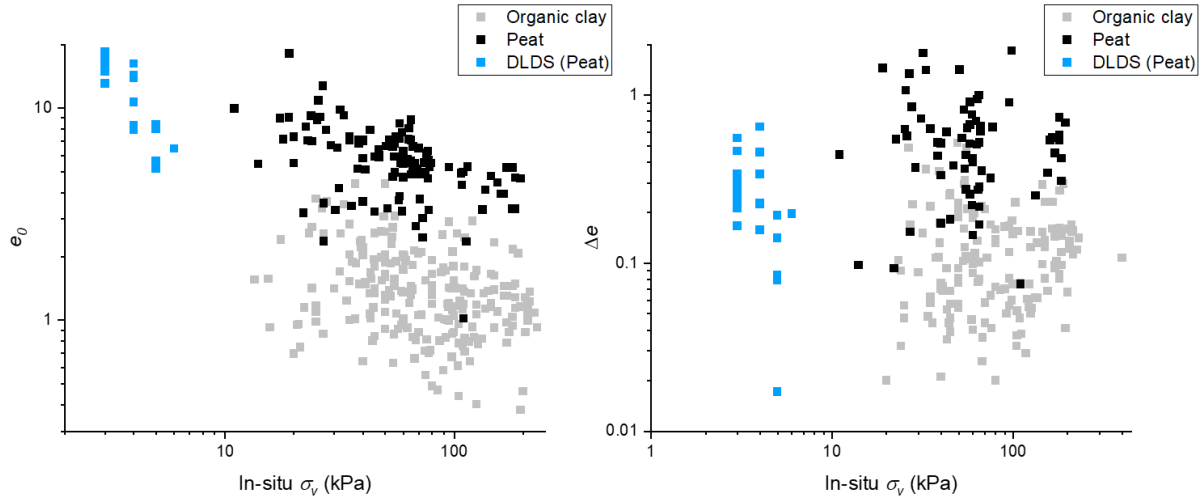
Figure 40. In-situ σ~v~ vs e~0~ (left) and in-situ σ~v~ vs Δe (right).

Following this, the influence of *w* on *RR* was plotted in Figure 41. While the CR is mainly used for engineering design applications involving settlement of soil, the *RR* is used in specific applications concerning soils of high OCR. As stated by Pirouzi and DeGroot (2019), the *RR* is strongly correlated with sample quality for clays, whereby the geotechnical parameter increases with more disturbance. Nevertheless, it is a complex parameter. While the maximum *w* in the DLDS database is 1183% based on 25 data points, the maximum *w* for Ackerman samples in the STOWA database is 721% based on 398 data points. In addition, even though organic clay shows a linear trend on the *w* (%) to RR plot, peat sampled by either the DLDS or Ackerman samplers show no correlation between these parameters. The relationship for organic clays is approximated with the linear equation 7. The adjusted R^2 (equation 8) is often used in conjunction with Pearson's 'r', and it is a statistical tool used to quantify the linear fitting capability of a trendline. The Pearson's 'r' and adjusted R^2 value are 0.849 and 0.718 respectively. For this linear relationship, the standard error for the slope and intercept were 110 and 3.82 respectively.

$$w = 1812 * RR + 7.44 \tag{7}$$

$$R^2_{adj} = 1 - \frac{RSS/df_{Error}}{TSS/df_{Total}} \tag{8}$$

With:

$RSS = \sum_{i=1}^{n}(y_i - \hat{y}_i)^2$

$TSS = \sum_{i=1}^{n}(y_i - \bar{y}_i)^2$

$\hat{y}$ = predicted value of y

$\bar{y}$ = mean of y-variable values

y_i = y-variable values of dataset

df_{Error} = the error of the degrees of freedom

df_{Total} = the total number of degrees of freedom

Due to the higher fraction of heavy minerals in clay, the relative density was higher for organic clay than for peat, as shown in Figure 42. An inverse relationship was observed as an increasing relative density resulted in an increased likelihood of a low *RR*, although this relationship was weaker, with a linear Pearson's 'r' of -0.75. This relationship can be explained by the *RR* dependence on strain, as

presented in equation 2. The dependence is such that the strain depends on the available pore space and *w*, which is lower for samples of higher relative density.
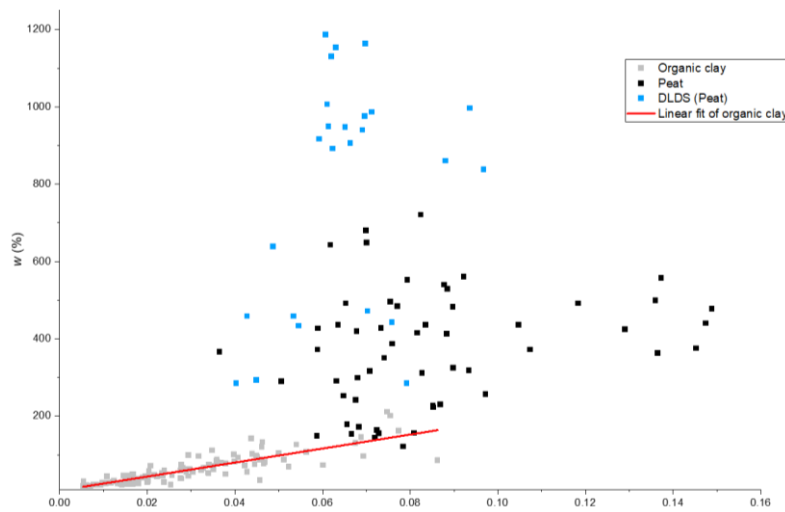
Figure 41. w vs RR plot.
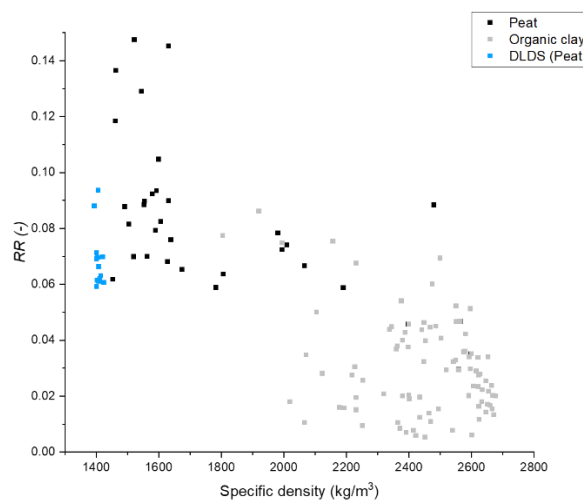
Figure 42. RR vs specific density plot

With increasing *w* a tendency of decreasing $\Delta e/e_0$ and a decrease of its variability was identified in Figure 43 (right). This trend can be explained by the much higher e_0 values typically found in peat. Likewise, the decreasing variability of $\Delta e/e_0$ in Figure 43 (right) with increasing *w* is due to the greatly increasing denominator in the disturbance index. Alternatively, the relationship can be explained by the fact that $\Delta e/e_0$ relies on the change in pore volume. As disturbance increases, the ability to swell and thus regain pore volume decreases, which results in a lower measure of *w*. The low $\Delta e/e_0$ variability in DLDS peats is likely due to the restriction to sampling in shallow soils. When disturbance parameters $\Delta e/e_0$ and *RR* are plotted against each other, as presented in Figure 43 (left), no agreement can be seen between them. This is in part due to these parameters being calculated from different phases of an IL oedometer test. Specifically, it is because the *RR* directly depends on both the σ_v' and $\Delta\varepsilon$, while $\Delta e/e_0$ depends only on the $\Delta\varepsilon$.
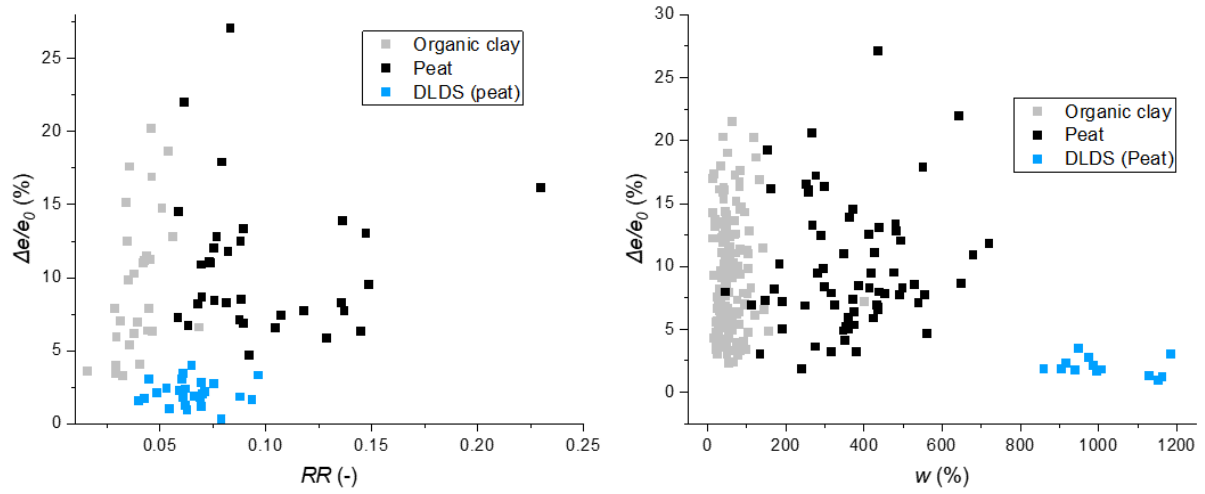
Figure 43. Δe/e0 vs water content (left) and Δe/e0 vs RR (right) plots.

6 Discussion

This thesis has used destructive and non-destructive methods to quantify disturbance in peats and organic clays. Peat remains a difficult soil to sample and performance of consistent 1D compression testing is challenging. Moreover, the difficulty of these operations increases with higher fibrousity, as with 'woody' peat (peats containing a high fraction of lightly decomposed twigs or branches) samples, which can cause jamming of the loading plate until the twig snaps due to the load. This sudden load transfer to the pore pressure greatly influences parameters derived from compression tests. In order to mitigate this, it is recommended to use a large consolidation cell, such as the Rowe consolidation cell due to the large compression potential of peat, which was not available for this investigation. Additionally, the diameter of these cells should be between 150 and 250 mm. However, this is not possible for Ackerman samples due to the diameter constraint of the tube, but different consolidation cell diameters may be used for DLDS specimens in future studies. The recommendation of using the conventional diameter to height ratio (D/H) range of three to four for oedometer specimens is not appropriate due to the aforementioned high compressibility of peat and potential presence of wood chips, therefore a D/H range of one to two is recommended. Additionally, peat is a sensitive soil to handle due to its low shear strength and high compressibility potential in an unconsolidated state. Adding to this fact, the DLDS is mostly deployed in shallow soils which have a very low σ_v'. Specimen loading in IL oedometer was challenging at times with these low σ_v' and low volumetric weight of samples, due to the old equipment available. A Large Direct Simple Shear Apparatus (LDSSA) and Large Diameter Triaxial Test (LDTT) have been developed by Deltares (Luijendijk, 2016) which utilizes samples from the DLDS. Therefore, alternatively to the proposed Rowe consolidation cell, the development of a new type of consolidation cell should be pursued having the diameter of a DLDS sample, i.e. 40 cm, ideally with CRS oedometer compatibility. In addition, it is often recommended by geotechnical sample preparation guidelines, such as the Manual of Soil Laboratory Testing (Head and Epps, 2011), to remove wooden lumps from samples, however this would not only induce disturbance to the sample, but also not represent in-situ conditions. This is inappropriate practice, and in addition, laboratory guidelines often allow filling of gaps in an oedometer cell with leftover soil pieces from the sample. This will not only decrease resemblance to in-situ structure, but also resemble a partially remoulded sample, which is known to be of higher disturbance. A great benefit of the DLDS is that due to its 40 cm diameter, which is six times larger than Ackerman tube diameter, more specimens can be prepared from a single depth level from one boring to account for lateral variability of the soil and test results. This is valid as long as standard laboratory sample dimensions are ensured. Another source of error is the influence of observation bias as experienced with t_{100} plots and the Casagrande method to find pre-consolidation pressure.

From the available literature on the use of radiography as a sample quality assessment method, qualitative analysis has been mostly conducted such as detailed by Ladd and DeGroot (2003), in order to identify disturbance features such as gas exsolution, wall shearing and the heterogeneity of void spaces near the ends of the tube. Due to these features being distinguishable at a macro level, a medical-CT scanner is sufficient for this qualitative method. While medical-CT scanners are an effective non-destructive method to identify the aforementioned disturbance features, the resolution is insufficient to provide insight into the degree of densification close to the sampler wall. In order to gain an insight into disturbance levels at a microscopic scale, the corresponding micro-CT scanner was used. However, quantitative analysis of the density changes with radial dependency of oedometer specimen analysis has not been done before, as the study by Ngan-Tillard et al (2016) focussed on the 1D compression

effects on archaeological remains such as seeds and mussels situated in peats and clays. While the study by Ngan-Tillard et al (2016) with a micro-CT scan of a peat oedometer specimen demonstrated that fibre compaction occurred together with the surrounding soil matrix, disturbance differences between samplers was not the objective of this study. With the micro-CT scans of peat from the SDT database, it was possible to demonstrate densification of specimens with increasing radial distance from the centre. Specimens A4pre and A4post had an increase in greyvalue intensity relative to the centre, a proxy measurement for density, of 10.97% and 12.28%, respectively. For DLDS specimens D4pre and D4post, this parameter was 1.49% and 1.82% respectively. This translates to the Ackerman specimen before consolidation having 7.4 times more densification in the outer 'skin' volume than the DLDS specimens. As this methodology was not encountered in the literature study, it must be further optimised and the trend that Ackerman specimens show more densification at the perimeter must be validated with additional scans on new specimens. It was not possible to convert greyvalue intensity into density due to a lack of reference material with known density in the scans. Although the conditions for all specimens which were scanned with the micro-CT were identical, it is unknown if and by how much the temperature increased within the micro-CT scanner during scanning. Even though the specimens were wrapped in plastic foil while scanning, the increased temperature within the micro-CT could have had an effect on densification levels as the evaporation rate of moisture on the specimen surface increases. Furthermore, the indistinguishableness between peat and water in micro-CT scans adds uncertainty as the quantity of each material cannot be accurately defined. A procedure aimed at increasing contrast between peat and water in scans done by replacing the water in peat with heavy water (deuterium oxide), which has a low attenuation coefficient, was deemed inappropriate, due to the disturbance induced to the specimen with the process of drying and rehydrating. Despite using the highest resolution settings on the micro-CT scanner, not all peat grain diameters from the sieve analysis (shown in of Figure 44 Appendix C) were larger than the highest resolution of 23 μm. In addition, due to the high angularity of peat grains, these grains have relative ease of interlocking with one another. This means that these grains might be accounted for as larger than they actually are during micro-CT scans and sieve tests. The experimental method of using micro-CT scans to quantify disturbance is a resource- and time-intensive method which is often not available for geotechnical sampling companies to conduct as part of sample quality designation procedures.

The modified $V_{v,b}/V_{SCPTU}$ disturbance method has shown that the Ackerman sample has a slightly higher V_s of 55.2 m/s compared to the 48.9 m/s of the DLDS, which means a 12.9% increased V_s. While these samples had a depth difference of 50 cm, both the SCPTU and MASW show fairly uniform V_s in the zone between the two sample depths, therefore negating any strong subsurface V_s heterogeneity effects. At the depth of interest, the confidence level of the MASW is ~100%, whereby the confidence is defined as the appropriateness of the modelled dispersion curve to the V_s change at a point in the cross-section. In addition, the relative standard error (RSE) of the respective bender element test differs due to the number of recorded tests, the Ackerman specimen had a 0.23% RSE and the DLDS had a 1.8% RSE. Therefore, the combination of these facts suggest that the difference in shear wave velocities between the samples is not due to soil heterogeneity, but rather due to densification of soil by the Ackerman sampling tube, leading to a higher degree of sample disturbance caused by the Ackerman sampler, compared to the DLDS.

The DLDS IL oedometer results from the Deltares database stem from shallow samples, the in-situ σ_v for these samples was 6 kPa or less, while the DLDS samples D3 and D4 from the SDT database had an in-situ σ_v' of 41.87 kPa. This highly contrasting in-situ σ_v may be the reason that $\Delta e/e_0$ was much more elevated in D3 and D4, at 35.4% and 39.4% respectively. The e_0 for D3 and D4 was comparable to other samples in the SDT dataset, while the Δe was an order of magnitude higher to the expected

value range. Other possible explanations may be that the yield stress is less than 10 kPa or that the low yield stress might have been breached due to swelling during transportation. Similarly to the findings of Boylan (2008) on Sherbrooke samples which showed very high w and water migration, the DLDS samples also show signs of water migration in samples, which causes an unequal distribution of w throughout the sample. The $\Delta e/e_0$ was plotted against in-situ σ_v for data from STOWA and Deltares, which showed that it becomes increasingly difficult to obtain organic clay or peat samples with a $\Delta e/e_0$ of less than 7% as in-situ σ_v increases. When observing only the STOWA data for samples with an $\Delta e/e_0$ under 7%, a threshold value of 155 kPa in-situ σ_v was established. While the trend of increasing $\Delta e/e_0$ with increasing in-situ σ_v is reasonable because of the large changes in confining pressure of samples from deeper soil layers, it is important to keep in mind that the $\Delta e/e_0$ was developed for marine clay samples with a plasticity index between 6% and 43%, a w between 20% and 67%, an OCR from one to four, and a depth up to 25 m below ground level. All DLDS samples from the Deltares database showed a $\Delta e/e_0$ of less than 4%. However, when separating the parameters within the $\Delta e/e_0$, it was apparent that the high e_0 values for the DLDS peat samples were lowering the aforementioned DLDS $\Delta e/e_0$ values below 4%. Meanwhile, the Δe component of the DLDS samples remained in the same range and variability as the peat and organic clay samples of the Ackerman sampler. Evidently, more DLDS IL oedometer results would be needed at the higher in-situ σ_v comparable to those of the Ackerman samples, however this is challenging due to the DLDS design to operate at shallow depths on peats which generally have a low volumetric weight. The RR, which may be used to measure disturbance, shows dependency on the specific density of organic samples with a weak negative correlation. This difference was expected due to the higher percentage of mineral content in organic clays compared to peats. The peats sampled by the DLDS have a lower specific density when compared to those gathered by STOWA with the Ackerman sampler. This is consistent with the higher w found in the DLDS sampled peats as well.

7 Conclusions

The main goal of this investigation was to explore how different sampling methods affect the derived soil properties and the consequent geotechnical design parameters in peats and organic clays. This was enabled by gathering existing data on tests from soils sampled by the Ackerman and DLDS samplers, in addition to the execution of conventional and non-conventional tests for sample disturbance quantification methods in the SDT database, i.e. difference in shear wave velocities, radiography and select parameters from IL oedometer testing.

Sub-question 1:
How does the DLDS affect consolidation parameters derived from (IL oedometer) laboratory tests in peats, when compared to traditional sampling techniques?

Differences were observed between organic clays and peats regarding the effect of sampler type on consolidation parameter *RR*. While organic clay has a clear linear trend between *w* and *RR*, peat shows no definitive correlation, although lower *w* levels were observed for the peats sampled by the Ackerman sampler than for the DLDS peats. This reinforces the notion that compared to the Ackerman sampler, the DLDS is more capable of retaining the *w* of samples and is therefore more representative of in-situ conditions.

Sub-question 2:
What is the relationship between sample disturbance and classification parameters (yield stress, density)?

Classification parameters were found to be heavily affected by disturbance. While 37% of Ackerman organic clay and peat samples have an $\Delta e/e_0$ below 7%, falling within the fair to excellent sample categories, the difficulty of obtaining undisturbed Ackerman samples increased with rising in-situ σ_v and therefore with depth. However, the high e_0 values of the DLDS samples decreased their respective $\Delta e/e_0$, inherently making these samples appear of less disturbance by this index. Specifically for peats, an elevated disturbance level measured by the *RR* did not indicate a drastically different specific density. Therefore, sample disturbance has the consequence of systematically misrepresenting geotechnical parameters in engineering design models, and must be measured by an appropriate disturbance parameter for the investigated soil.

Sub-question 3:
How do the properties (density and shear wave velocity) of peat samples derived from CT scans and bender element testing* compare when different samplers are used?

Densification observed by micro-CT scans around the perimeter of oedometer specimens were different between the two samplers compared. The Ackerman specimen scanned before consolidation had a 7.4 times higher densification in the outer 'skin' volume than the DLDS specimen before consolidation. The $V_{s,b}$ was 12.9% higher for the Ackerman peat sample when compared to the DLDS sample at the same site in Gouda, which were respectively 65.4% and 54.4% higher than the in-situ V_{SCPTU}. Using the SCPTU and bender element testing method, it was concluded that the higher value of $V_{s,b}$ of the Ackerman sampler is due to the densification near the perimeter of the sample as observed by the micro-CT scans.

Main research question:
How does sampling affect soil properties and the consequent geotechnical design parameters?

Sampling affects soil properties by altering the water content, stress states, density and chemistry of the soil compared to in-situ conditions. The larger diameter of the DLDS ensures more water content retention when compared to the Ackerman sampler, which in turn influences geotechnical parameters such as the *RR*. The diameter of the DLDS also renders more of the volume from the block as undisturbed, unlike the Ackerman sampler which showed higher densification around the skin of specimens as a result due to the friction of the tube wall. The first main conclusion is that the DLDS is more suitable for sampling in shallow peat, compared to the Ackerman sampler. The second main conclusion is that the radiography and shear wave velocity results from this study have shown that sample disturbance with peats may be better quantified and assessed with non-destructive methods. Yet, the number of samples these methods were conducted on are insufficient to firmly advise that non-destructive testing for sample quality assessment is necessary in the geotechnical sampling industry.

8 Recommendations

For future studies related to the topic of this thesis, it is advised to use CRS oedometer apparatus rather than the standard IL oedometer, due to the ability of the CRS oedometer to conduct strain controlled compression, which is greatly preferred due to the continuously changing strain in 1D compression tests. In addition, if the method detailed in this study, of CT scanning a consolidated specimen is used, it is proposed to develop a consolidation cell which maintains the load after the final loading stage on the specimen, enabling the scan of the specimen maintained at the desired σ_v'. This device must be of low density material, i.e. plastic, in order not to cause the beam hardening effect observed when scanning metals such as steel. It would be of interest to use the futural new micro-CT scanner in the Civil Engineering and Geosciences department of TU Delft, whereby sufficient space will be available within the scanner to accommodate a CRS (or IL) oedometer rig within it. In this way, the sample can be loaded during scanning to not only capture the orientation changes of peat fibres, but also regional densification throughout the 1D consolidation process. However, this method will need rapid scanning settings, which will entail a decreased resolution due to the continually changing configuration of grains in specimens. If this method can be accomplished, it is encouraged to develop an experimental setup whereby an Ackerman sampling tube is penetrating a DLDS sampled block while making a CT scan, either with the medical-CT or micro-CT scanner, in order to observe the edge effect of the tube on the soil in different phases. Appropriate steps such as sufficient lateral support of the DLDS block must be taken if this method is pursued. The aforementioned setup will also enable the comparison in density changes of the exact same soil portion before and after using the Ackerman tube to sample the DLDS block.

As argued in section 3.3, the Ackerman sampler falls short by 3 mm of the required minimum inner diameter of samples needed in order to be classified as appropriate for sampling organic clays and peats for category A samples. For the sampling industry in the Netherlands, it is therefore advised to increase the inner diameter of Ackerman tubes to between 70 mm and 120 mm and use a length of 600 mm such that category A samples are achieved.

It is highly recommended to gather more IL oedometer DLDS data, as deployment of the sampler continues. This will alter the reliability of the results and reasonings discussed in this thesis. In addition, it is encouraged to repeat the SCPTU test with the APvdBerg system, as the failure detailed in section 4.4 resulted in no shear wave velocity readings to compare to the Geomill system at the desired depth. This will enable a more comprehensive analysis of the difference of using these systems for non-destructive disturbance testing quantification. Moreover, further shear wave velocity comparison tests should be made using the methods described in sections 4.2 and 5.1.3 to further demonstrate the applicability of this method in organic soils. Results from the micro-CT image analysis method should be reproduced in order to confirm the trend of higher densification observed with increasing radial distance from the centre for Ackerman samples. Specimen temperature rose till 26.5°C during pycnometer testing, while micro-CT scanning increased specimen's temperature by an unknown quantity, which may have degraded the organic matter present in the specimens. It is important to determine whether this has an effect on the structure of peats. Therefore, it is advised for geotechnical sampling companies to use the DLDS to sample shallow peats and to treat disturbance quantification of peat samples differently than before.

Challenges occur when comparing different samplers used at different site locations because variables such as the depth of the ground water table play a fundamental role in comparing disturbance of samples. In this investigation, no sampling site had both the use of the Ackerman sampler and DLDS for a side-by-side comparison. As this set-up is highly valuable for limiting variables, it is recommended to increase the number of occasions this opportunity occurs. Finally, while higher water contents in peat samples are representative of in-situ conditions, the study by Boylan et al. (2008) and the results from this thesis have shown that high water content lead to water migration within the sample in its respective container, which will lead to different specimen properties depending on the location the specimen is extracted from within the sample. This may be mitigated by a suction device within the sample tube, which can keep the water content distribution constant throughout the sample.

9 References

Amundsen et al. (2015). "Comparison of two sample quality assessment methods applied to oedometer test results". *IOS Press*, 923-930, DOI: 10.3233/978-1-61499-601-9-923.

Andresen, A. and Kolstad, P. (1979). "The NGI 54-mm samplers for undisturbed sampling of clays and representative sampling of coarser materials". *Proceedings of the International Symposium of Soil Sampling, State of the Art on Current Practice of Soil Sampling*, 13-23.

ASTM International. (2005). "Standard Guide for Selection of Soil and Rock Sampling Devices Used With Drill Rigs for Environmental Investigations". *ASTM D6169 – 98*, West Conshohocken, Pennsylvania, United States.

ASTM International. (2018). "Standard Practices for Obtaining Intact Block (Cubical and Cylindrical) Samples of Soils". *ASTM D7015/D7015M*, West Conshohocken, Pennsylvania, United States.

Baligh et al. (1987). "Disturbances due to ideal tube sampling". *Journal of Geotechnical Engineering* Volume 113 Issue 7.

Boylan, N. (2008). "The Shear Strength of Peat". *University College Dublin*.

Clayton et al. (1998). "Effects of sampler design on tube sampling disturbance - numerical and analytical investigations". *Géotechnique 48, No. 6*, 847-867.

Chung, S. and Kweon, H.J. (2013). *Oil-Operated Fixed-Piston Sampler and Its Applicability*. [diagram]. https://www.researchgate.net/publication/264862318_Oil-Operated_Fixed-Piston_Sampler_and_Its_Applicability

CUR (2005). "Uitvoering en Interpretatie samendrukkingsproef". Aanbeveling 101. *CUR*.

DeGroot et al (2005). "Sample disturbance – soft clays". *Studia Geotechnica et Mechanica.* Vol. 27 Issue 3/4, p91-105. 15p.

Deltares (2020). "Extra grote veenmonsters om bodemdaling te voorspellen" [Photograph]. https://www.h2owaternetwerk.nl/h2o-actueel/extra-grote-veenmonsters-om-bodemdaling-te-voorspellen

Dong et al. (2016). "Dependencies of Shear Wave Velocity and Shear Modulus of Soil on Saturation". *Colorado School of Mines*.

Donohue, S. and Long, M., (2010). "Assessment of sample quality in soft clay using shear wave velocity and suction measurements". *Géotechnique*. 60(11), 883-889.

Ferreira et al. (2011). "Shear wave velocities for sample quality assessment on a residual soil". *Japanese Geotechnical Society*. Vol. 51, No. 4, 683-692.

Head, K. H. and Epps, R. J. (2011). "Manual of Soil Laboratory Testing". *Whittles Publishing*. Vol. 2 Ch. 14.

Helenelund et al. (1972). "Influence of sampling disturbance on the engineering properties of peat samplings". *Proceedings of the international peat congress*. 229-240.

Karlsrud K., Hernandez-Martinez, F.G. (2014). "Strength and deformation properties of Norwegian clays from laboratory tests on high-quality block samples*". Canadian Geotechnical Journal.* 50(12): 1273-1293. https://doi.org/10.1139/cgj-2013-0298

Konrad, J.-M., Gilbert, F., Pouliot, N., and Saint-Laurent, S.1995a. "Large diameter sampling of sands". CANLEX Technical Report, Phase II, Activity 4C, *Université Laval, Sainte-Foy.*

La Rochelle, P., Sarrailh, J., Tavenas, F., Roy, M., and Leroueil, S.1981. "Causes of sampling disturbance and design of a new sampler for sensitive soils". *Canadian Geotechnical Journal,* 18: 52–66.

Lacasse, S. and Berre, T. (1988). "State-of-the-Art: Triaxial testing methods for soils*". ASTM International STP29081S, 264-289.* DOI: 10.1520/STP29081S.

Ladd C.C., DeGroot D.J. (2003). "Recommended practice for soft ground site charaterization: Arthur Casagrande Lecture*". 12th Panamerican Conference on Soil Mechanics and Geotechnical Engineering*.

Ladd, C.C., Azzouz, A.S., Martin, R.T., Day, R.W., and Malek, A.M., (1980). "Evaluation of the compositional and engineering properties of offshore Venezuelan soils". *M. Dept. of Civil Engr.*

Ladd C.C., DeGroot D.J. (2003). "Recommended practice for soft ground site charaterization: Arthur Casagrande Lecture*". 12th Panamerican Conference on Soil Mechanics and Geotechnical Engineering*.

Landon et al. (2007). "Nondestructive Sample Quality Assessment of a Soft Clay Using Shear Wave Velocity*". Journal of Geotechnical and Geoenvironmental Engineering 133(4).*

Luijendijk, S. (2016). "Deltares Large Diameter Sampler resultaten". *Deltares.*

Lunne et al. (1997). "Sample disturbance effects in low plastic Norwegian clay". *Canadian Geotechnical Journal, 43, 726-750.*

Mayne et al. (2009). "State-of-the-art paper (SOA-1): geomaterial behavior and testing*". Conference: 17th International Conference on Soil Mechanics and Geotechnical Engineering Volume 4.*

Ministry of Infrastructure and Water Management (2016). "Samendrukkingsproeven". *Schematiseringshandleiding macrostabiliteit*. The Hague, Netherlands.

Ngan-Tillard et al. (2016). "Tools for Predicting Damage to Archaeological Sites Caused by One-Dimensional Loading" *Conservation and Management of Archaeological Sites*, 18:1-3, 70-85, DOI: 10.1080/13505033.2016.1181934

NEN (1989). "Geotechnics - Classification of unconsolidated soil samples". (NEN 5104:1989 nl). *NEN*.

NNI (2018). "Geotechnical investigation and testing - Sampling methods and groundwater measurements - Part 1: Technical principles for the sampling of soil, rock and groundwater.*"* (NEN-EN-ISO 22475-1:2021). *ISO*. Geneva, Switzerland.

NNI (2021). "Geotechnical investigation and testing - Sampling methods and groundwater measurements - Part 1: Technical principles for the sampling of soil, rock and groundwater." (NEN-EN-ISO 22475-1:2021). *ISO*. Geneva, Switzerland.

Nordmeyer (n.d.). "HBS". Hollow stem auger system. [image] http://www.nordmeyer.nl/membersonly/HBS%20english.pdf

Pirouzi, A. and DeGroot, D. (2019). "Evaluation of recompression index for structured clays from laboratory constant rate of strain consolidation tests". *GeoEngineers, Inc.,* San Diego, CA, USA.

Tanaka, H. (1996). "Characteristics of Drammen clay measured by Port and Harbour Research Institute (PHRI), Japan". *Port and Harbour Research Institute.*

Tanaka, H., (2000). "Sample quality of cohesive soils : Lessons from three sites, Ariake, Bothkennar and Drammen". *Soils and foundations*. 20(4), 57-74.

TAW. (2001). "Bijlage 3, Boringen". *Technisch Rapport Waterkerende Grondconstructies.* 263-265.

Van Essen, H. (2021). "Wandwrijving samendrukkingsproef". *Deltares*.

Wride et al. (2000). "Ground sampling program at the CANLEX testsites". *Canadian Geotechnical Journal*, 37, 530-542.

Zwanenburg, C. (2017a). "Development of a Large Diameter Sampler". *Proceedings of the 19th International Conference on Soil Mechanics and Geotechnical Engineering.* Seoul, South Korea.

Zwanenburg, C. (2017b). "SBRCURnet kwaliteit van grondonderzoek (monsterverstoring veen)". [presentation]. *Deltares*.

Appendices

A Pycnometer results

The results of the pycnometer test, which was used to establish a *G* value for every sample, are shown in Table 13.

Table 13: Pycnometer test results

Specimen name	Input mass (g)	Average volume (cm^3)	Average density (g/cm^3)	Standard deviation of density (g/cm^3)
D1/D2	16.3400	10.2015	1.6017	0.0014
A1/A2	55.3800	23.7801	2.3288	0.0068
A3/A4	17.6700	10.1519	1.7406	0.0043
D3/D4	16.7100	13.0560	1.2799	0.0021

B SCPTU shear wave velocities

The SCPTU test, which measures the in-situ shear wave velocity at different depths, is shown in Table 14 by the two different systems used.

Table 14: SCPTU shear wave velocities by measurement system.

Interval (m)	Geomill system shear wave velocity (m/s)	APvdBerg system shear wave velocity (m/s)	Difference between Geomill and APvdBerg systems (%)
1.0 – 1.5	87	84	3.51
1.5 – 2.0	71	89	22.5
2.0 – 2.5	83	51	47.8
2.5 – 3.0	30	47	44.2
3.0 – 3.5	84	29	97.3
3.5 – 4.0	29	25	14.8
4.0 – 4.5	19	29	41.7
4.5 – 5.0	27	-	
5.0 – 5.5	28	-	
5.5 – 6.0	28	-	
6.0 – 6.5	48	-	
6.5 – 7.0	51	-	
7.0 – 7.5	46	-	
7.5 – 8.0	42	-	
8.0 – 8.5	40	-	
8.5 – 9.0	40	-	
9.0 – 9.5	63	-	
9.5 – 10.0	127	-	
10.0 – 10.5	121	-	
10.5 – 11.0	153	-	

C   Wet sieve analysis results

The intention of the wet sieve analysis on peat sample VN80625-1-1 was to gain an insight into the grain size distribution and the appropriateness of the applied maximum micro-CT resolution of 23 μm.
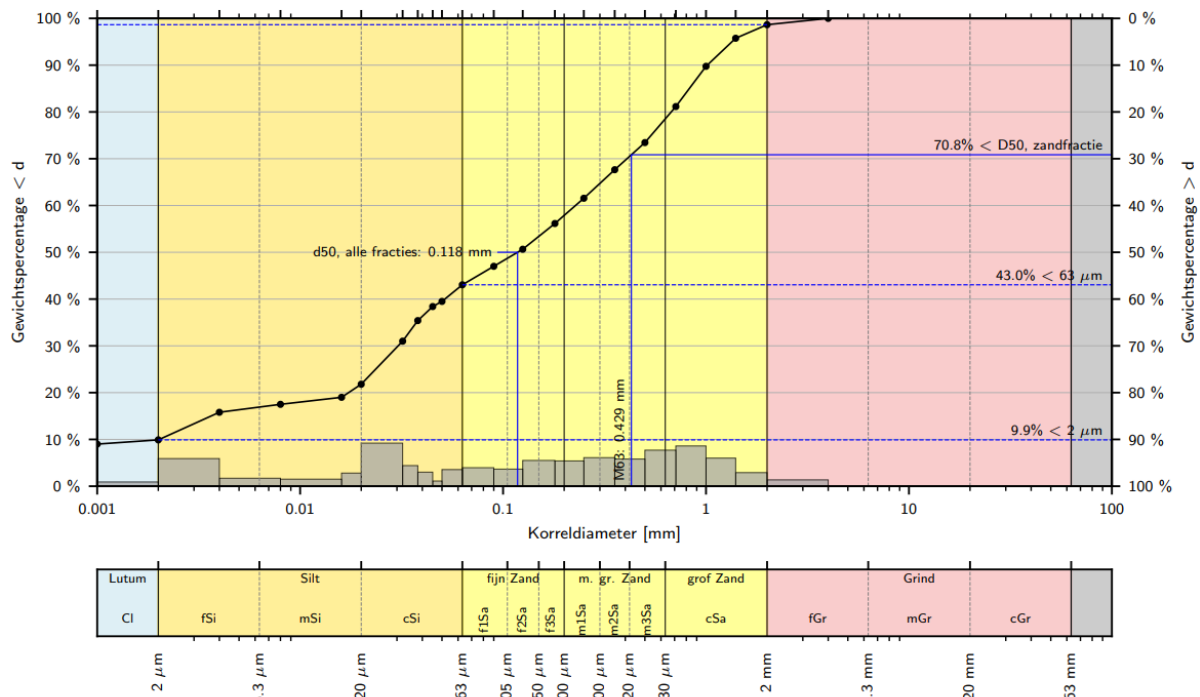
Figure 44. Wet sieve analysis result for sample VN80625-1-1.

D   Image analysis script

Table 15 details the commands used to analyse the specimens scanned by the micro-CT scanner. The known components of the samples are a majority of water filled pores, peat, air filled pores and sand grains. A computer with 32GB RAM was used due to the large image files and processing power demand. The following installed plugins are required in ImageJ before starting analysis: Concentric circles, Z Project Ignore NaNs.

Table 15. Image analysis methodology.

Action	Meaning	Comments
File -> import -> image sequence -> "A4post"	Get a new file for analysis	
Image -> adjust -> threshold Use 6635-65535 thresholding range (Off) Calculate threshold for each image, then apply	This range is for all the solids and liquid in the specimen	Will create a binary image stack whereby the volume of interest will be ones and the background will be zeros
Process -> binary -> fill holes	Fills the pores in the specimen with 1s	Will fill the air pores within the sample

Process -> binary -> options Iterations: 20 Black background: v Do: Open	Now we have the volume of interest of the specimen	Makes an erosion operation, followed by dilation in order to remove the outer ring.
File -> Save -> name: "A4postVolumeofInterest"		
File -> import -> image sequence -> "A4post"		
Image -> adjust -> threshold Use 12606-65535 thresholding range (Off) Calculate threshold for each image, then apply	This is the greyvalue intensity range for the high density silica in the specimen	Will create a binary image stack whereby the silica grains will be ones and the rest will be zeros.
File -> Save -> name: "A4postSilica"		
File -> import -> image sequence -> "A4post"		
Image -> adjust -> threshold Use 1-6635 thresholding range (Off) Calculate threshold for each image, then apply	The thresholding values range for the macro pores in the specimen	Will create a binary image stack whereby the pores in the peat will be ones and the rest will be zeros.
File -> Save -> name: "A4postMacropores"		
File -> import -> image sequence -> "A4post"		
Process -> image calculator Image1: "A4postVolumeofInterest" Operation: min Image2: "A4post"	Overlaying greyvalues onto the volume of interest	
File -> Save -> name: "A4postVolumeInterest+greyvalues"		
Process -> image calculator Image1: "A4postVolumeInterest+greyvalues" Operation: subtract Image2: "A4postSilica"	Removing silica material from image stack	
File -> Save -> name: "A4postMinusSilica"		
Process -> image calculator Image1: "A4postMinusSilica" Operation: subtract Image2: "A4postMacropores"	Removing macro pores from image stack	The resulting image stack will be only the greyvalue intensity for the organic matter and water in peat.
File -> Save -> name: "A4postpeat"	This image is now in 8-bit due to the aforementioned operations, which involved several 8-bit binary image stack, downgrading the 16-bit	For A4post -> 8-bit greyvalues: silica ~200, air: ~25, peat: ~37

Image -> Type -> 32-bit	Converting to 32-bit which is needed for the later step of changing the zeros to NaNs.	This will not scale the greyvalues from 8-bit.
Image -> Adjust -> Threshold Use 1-1e30 NO apply	Selecting the peat and not the background, in order to set zeros to NaNs.	
Process -> Math -> NaN Background	The zeros will be set to NaNs, which is needed as only the organic matter and water in peat must be analysed when making the Z projection.	
Reset threshold		
Plugins -> Z Project Ignore NaNs	An average intensity along the Z axis is calculated and projected onto one image file.	This operation does not have a status bar and processing can take some time.
File -> Save -> name: "A4postProjection"		
Plugins -> Concentric Circles Number of circles: 200 Inner radius: 10 Adjust coordinates to the centre of the specimen accordingly Measure: v Ok	An average intensity is calculated along the perimeter of each circle, for each radius size, displayed in the pop up results window.	
Copy data from popup window to excel	Graph distance to centre (x axis) vs greyvalue intensity (y axis).	
Using the image stack named "A4postpeat" again for the following (similar) steps to calculate the standard deviation at each point:		
Image -> Adjust -> Threshold Use 1-1e30 NO apply	Selecting the peat and not the background, in order to set zeros to NaNs.	
Process -> Math -> NaN Background	The zeros will be set to NaNs, which is needed as only the organic matter and water in peat must be analysed when making the Z projection.	
Reset threshold		
Image -> stacks -> Z Project Projection type: standard deviation	The resulting single image will have standard deviation values calculated	

	along the z-axis of the specimen	
File -> Save -> name: "A4postSDTProjection"		
Plugins -> Concentric Circles Number of circles: 200 Inner radius: 10 Adjust coordinates to the centre of the specimen accordingly Measure: v Ok	An average standard deviation is calculated along the perimeter of each circle, for each radius size, displayed in the pop up results window.	
Copy data from popup window to excel	Add to data after converting to relative standard error (RSE) as uncertainty measurement	
The same steps above are used to calculate the greyvalue intensity for the other three scans, substituting with use of the appropriate file naming: A4pre, D4post and D4pre. The threshold ranges for these specimens are listed in Table 16 .		

Table 16: Threshold ranges and iterations for different phases per specimen.

Specimen name	Volume of interest threshold	Iterations	Silica threshold	Pores threshold
A4post	6635-65535	20	12606-65535	1-6635
A4pre	8493-65535	5	15714-65535	1-8493
D4post	5480-65535	6	7499-65535	1-5480
D4pre	6202-65535	5	9004-65535	1-6202

Table 17: Peak greyvalue intensity values from greyvalue histograms by phase type per specimen.

Specimen name	Image bits	Air peak	Peat peak
A4post	16	~5287	~8812
	8	24	40
A4pre	16	~6886	~10820
	8	34	55
D4post	16	~4884	~6321
	8	35	44
D4pre	16	~5381	~7573
	8	28	40

E   SDT IL oedometer data

The full list of properties and parameters from the IL oedometer tests in the SDT database can be found in Table 18.

Table 18: Full dataset of IL oedometer tests in SDT database (continued on next page).

Sample name	Specimen name	Soil type	Ring I.D. (mm)	Ring height (mm)	Soil mass before testing (g)	Soil mass after testing (g)	Sampling method	Volumetric weight (kN/m3)	σ_v' (kPa)	Depth (m)	Location	1st Loading step (kg)	2nd Loading step (kg)	3rd Loading step (kg)	4th Loading step (kg)
11204108	D1	Peat	65	29.5	94.9	83.0	DLDS	14	5.6	1.4	Vlist	0.46	0.93	1.86	3.72
11204108	D2	Peat	65	19.5	71.1	60.08	DLDS	14	5.6	1.4	Vlist	0.46	0.93	1.86	3.72
2A 3 2	A1	Organic clay	65	29.5	136.3	99.9	Ackerman	15.1	13.94	2.75	Vlist	1.16	2.31	4.63	9.25
2A 3 2	A2	Organic clay	65	19.5	90.1	88.34	Ackerman	15.1	13.94	2.75	Vlist	1.16	2.31	4.63	9.25
2C 5 2	A3	Peat	65	19.5	70.1	44.5	Ackerman	11.1	9.7	2.5	Vlist	0.80	1.61	3.22	6.44
2C 5 2	A4	Peat	65	29.5	108.4	70.6	Ackerman	11.1	9.7	2.5	Vlist	0.80	1.61	3.22	6.44
VX-80625-1	D3	Peat	65	19.5	62.1	23.3	DLDS	9.5	41.87	5.06	Gouda	3.47	6.95	13.89	27.79
VX-80625-1	D4	Peat	65	29.5	93.0	35.8	DLDS	9.5	41.87	5.06	Gouda	3.47	6.95	13.89	27.79

Specimen name	5th Loading step (kg)	6th Loading step (kg)	7th Loading step (kg)	8th Loading step (kg)	9th Loading step (kg)	G	Dry volumetric weight (kN/m3)	e_0	Δe	$\Delta e/e_0$	Pre-consolidation stress s (kPa)	In-situ σ_v' (kPa)	OCR	Initial volumetric w (%)	RR (Casagrande)	RR (Taylor)
D1	7.43	3.72	7.43	18.58	-	1.6	2.75	4.8	0.412	8.55	11.2	5.6	2	305	-	0.056
D2	7.43	3.72	7.43	18.58	-	1.6	2.75	4.8	0.433	8.99	11.2	5.6	2	305	-	0.103
A1	18.51	9.25	18.51	46.27	74.02	2.33	6.34	2.7	0.221	8.26	28	13.9	2	173	0.020	0.018
A2	18.51	9.25	18.51	46.27	74.02	2.33	6.34	2.7	0.195	7.29	32	13.9	2.3	173	0.016	0.014
A3	12.88	6.44	12.88	25.75	51.50	1.74	2.98	4.8	0.307	6.35	15	9.7	1.5	308	-	0.028
A4	12.88	6.44	12.88	25.75	51.50	1.74	2.98	4.8	0.255	5.26	21	9.7	2.2	308	0.030	0.027
D3	55.58	27.79	55.58	111.15	222.30	1.28	2.90	3.4	1.21	35.4	20.935	41.9	0.5	254	0.045	0.012
D4	55.58	27.79	55.58	111.15	222.30	1.28	2.90	3.4	1.35	39.4	31.5	41.9	0.8	254	0.260	0.217